eyes with an ERM. This means that the distance between each scan line should be set to less than 75 μm in the Cirrus HD-OCT. For example, the consecutive OCT images of case 5 were obtained with 5-line scans with a distance between the scans of 20 μm (Fig 3A, bottom). Moreover, because the fixation point is sometimes shifted upward in cases of longstanding ERM, the OCT scan should be repeated until the true center of the fovea is scanned.

The cotton ball sign in the OCT images seemed to be strongly correlated with the inward traction on the retina. In eyes with VMT, local adhesions between the vitreous and retinal surface causes strong and direct inward traction over the entire depth of the foveal pit.[13,16] However, an ERM causes a tangential shrinkage of the retinal surface, and this leads to an inward retinal displacement of the fovea, regardless of the existence of a posterior vitreous detachment. This continuous tension also affects the photoreceptor layer, leading to mechanical damage of the photoreceptors and deterioration of visual function.[12,14,15] In this study, in eyes with VMT in which direct vitreous traction was present at the fovea, the cotton ball sign was always observed, although there was no apparent inward displacement of the fovea in cases 1 through 5 (Figs 1 and 3) and the CFT was normal, except in cases 6 and 7 (Table 1, available at http://aaojournal.org). In the eyes with an ERM, the mean CFT of the cases with the cotton ball sign was significantly thicker than that in eyes without the cotton ball sign (Table 2). These findings indicate that the continuous inward traction by the ERM was the cause of the cotton ball sign. In 8 of 16 cases that underwent vitrectomy, the cotton ball sign disappeared within 6 months and the CFT was significantly thinner than that in eyes where the cotton ball sign did not disappear. This indicated that disappearance of the highly reflective region was not the result of the removal of the ERM, but was most likely the result of the release of inward traction. It is notable that in cases where the cotton ball sign disappeared after surgery, the foveal pit reappeared because of release of inward traction (Fig 2B, cases 39, 43, and 44). However, in cases where the cotton ball sign did not disappear, the foveal area was still flat or even convex (Fig 2B, cases 40, 41, and 42). These highly reflective regions were observed only at the foveal center, even in cases where the entire macular region was thickened because of the ERM. There are 2 possible reasons for why the cotton ball sign is observed only at the foveal center in the ERM eyes. First, in cases in which the internal limiting membrane became flat because of the tangential traction by the ERM, the inward traction could be applied most strongly to the photoreceptors at the foveal center because of the presence of the foveal pit. Second, the cone photoreceptors at the fovea have an elongated shape and their diameter is much smaller than those at the parafoveal region. This characteristic anatomic structure makes them more susceptible to the minute structural changes that may lead to the increased reflectivity in the OCT.

An ERM usually is associated with macular edema and reduced reflectivity resulting from fluid accumulation; however, an increase in the reflectivity is observed rarely. Then the question arises on why the inward traction affected the reflectivity of the foveal center in the OCT images? The highly reflective region was always located between the IS/OS junction and COST lines. This region corresponds to the outer segment of cone photoreceptors, whose reflectivity is usually low. The photoreceptor outer segments (OSs) contain stacks of membranous discs that are rich in visual pigments, and the OSs are aligned parallel to the light pathway. The authors suggest that the inward traction on the retina changes the alignment of the OSs, which then increases their reflectivity. Directional reflectivity is known to exist in the retinal nerve fiber layer[21,22] and Henle's fiber layer.[23] Recently, Lujan et al[23] successfully distinguished Henle's fiber layer from the true outer nuclear layer by varying the angular incidence of the OCT beam on the retinal plane. The photoreceptor OSs are long cylindrical structures whose reflectivity may depend on the angular incidence of the OCT beam.

The second hypothesis for the highly reflective region is that the continuous inward traction causes microstructural damages to the cone OSs, leading to glial migration, glial scar formation, and photoreceptor degeneration.[24] However, it is not likely that these changes could be reversible and, particularly in case 5, would completely recover within 30 days after the release of mechanical traction (Fig 3, case 5).

The exact mechanism causing the highly reflective region was not determined, but there is very little possibility that this highly reflectivity region is an optical artifact, because it appeared when inward traction was forced to the outer retina, regardless of the existence of an ERM, and disappeared when the traction was released.

The cotton ball sign was present, despite good vision in the patients; 4 of 7 eyes with VMT and 9 of 30 eyes with an ERM with the cotton ball sign had best-corrected visual acuity of 0.8 or better (Table 1, available at http://aaojournal.org). This means that the cotton ball sign does not necessarily indicate a decrease in visual acuity, and it may be used as a predictor of visual impairment that would arise after longstanding inward traction at the fovea. Continuous foveal traction is known to cause microstructural damages in the photoreceptor layer,[12–16] and early detection of this sign may help in the management of these patients in preserving good vision.

References

1. Jaffe NS. Vitreous traction at the posterior pole of the fundus due to alterations in the vitreous posterior. Trans Am Acad Ophthalmol Otolaryngol 1967;71:642–52.
2. Wise GN. Relationship of idiopathic preretinal macular fibrosis to posterior vitreous detachment. Am J Ophthalmol 1975; 79:358–62.
3. Smiddy WE, Maguire AM, Green WR, et al. Idiopathic epiretinal membranes: ultrastructural characteristics and clinicopathologic correlation. Ophthalmology 1989;96:811–20; discussion 821.
4. Gandorfer A, Rohleder M, Kampik A. Epiretinal pathology of vitreomacular traction syndrome. Br J Ophthalmol 2002;86: 902–9.
5. Puliafito CA, Hee MR, Lin CP, et al. Imaging of macular diseases with optical coherence tomography. Ophthalmology 1995;102:217–29.

6. Wilkins JR, Puliafito CA, Hee MR, et al. Characterization of epiretinal membranes using optical coherence tomography. Ophthalmology 1996;103:2142–51.
7. Meyer CH, Rodrigues EB, Mennel S, et al. Spontaneous separation of epiretinal membrane in young subjects: personal observations and review of the literature. Graefes Arch Clin Exp Ophthalmol 2004;242:977–85.
8. Johnson MW. Tractional cystoid macular edema: a subtle variant of the vitreomacular traction syndrome. Am J Ophthalmol 2005;140:184–92.
9. Schmidt-Erfurth U, Leitgeb RA, Michels S, et al. Three-dimensional ultrahigh-resolution optical coherence tomography of macular diseases. Invest Ophthalmol Vis Sci 2005;46:3393–402.
10. Legarreta JE, Gregori G, Knighton RW, et al. Three-dimensional spectral-domain optical coherence tomography images of the retina in the presence of epiretinal membranes. Am J Ophthalmol 2008;145:1023–30.
11. Koizumi H, Spaide RF, Fisher YL, et al. Three-dimensional evaluation of vitreomacular traction and epiretinal membrane using spectral-domain optical coherence tomography. Am J Ophthalmol 2008;145:509–17.
12. Michalewski J, Michalewska Z, Cisiecki S, Nawrocki J. Morphologically functional correlations of macular pathology connected with epiretinal membrane formation in spectral optical coherence tomography (SOCT). Graefes Arch Clin Exp Ophthalmol 2007;245:1623–31.
13. Gaudric A. Macular cysts, holes and cavitations: 2006 Jules Gonin lecture of the Retina Research Foundation. Graefes Arch Clin Exp Ophthalmol 2008;246:1071–9.
14. Suh MH, Seo JM, Park KH, Yu HG. Associations between macular findings by optical coherence tomography and visual outcomes after epiretinal membrane removal. Am J Ophthalmol 2009;147:473–80.
15. Falkner-Radler CI, Glittenberg C, Hagen S, et al. Spectral-domain optical coherence tomography for monitoring epiretinal membrane surgery. Ophthalmology 2010;117:798–805.
16. Takahashi A, Nagaoka T, Ishiko S, et al. Foveal anatomic changes in a progressing stage 1 macular hole documented by spectral-domain optical coherence tomography. Ophthalmology 2010;117:806–10.
17. Odrobina D, Michalewska Z, Michalewski J, et al. Long-term evaluation of vitreomacular traction disorder in spectral-domain optical coherence tomography. Retina 2011;31:324–31.
18. Tsunoda K, Fujinami K, Miyake Y. Selective abnormality of cone outer segment tip line in acute zonal occult outer retinopathy as observed by spectral domain optical coherence tomography. Arch Ophthalmol 2011;129:1099–101.
19. Srinivasan VJ, Monson BK, Wojtkowski M, et al. Characterization of outer retinal morphology with high-speed, ultrahigh-resolution optical coherence tomography. Invest Ophthalmol Vis Sci 2008;49:1571–9.
20. Fernandez EJ, Hermann B, Povazay B, et al. Ultrahigh resolution optical coherence tomography and pancorrection for cellular imaging of the living human retina. Opt Express [serial online] 2008;16:11083–94. Available at: http://www.opticsinfobase.org/abstract.cfm?URI=oe-16-15-11083. Accessed August 9, 2011.
21. Knighton RW, Huang XR. Directional and spectral reflectance of the rat retinal nerve fiber layer. Invest Ophthalmol Vis Sci 1999;40:639–47.
22. Knighton RW, Qian C. An optical model of the human retinal nerve fiber layer: implications of directional reflectance for variability of clinical measurements. J Glaucoma 2000;9:56–62.
23. Lujan B, Roorda A, Knighton RW, Carroll J. Revealing Henle's fiber layer using spectral domain optical coherence tomography. Invest Ophthalmol Vis Sci 2011;52:1486–92.
24. Schuman SG, Koreishi AF, Farsiu S, et al. Photoreceptor layer thinning over drusen in eyes with age-related macular degeneration imaged in vivo with spectral-domain optical coherence tomography. Ophthalmology 2009;116:488–96.

Footnotes and Financial Disclosures

Originally received: March 17, 2011.
Final revision: June 20, 2011.
Accepted: August 11, 2011.
Available online: November 23, 2011. Manuscript no. 2011-444.

[1] Laboratory of Visual Physiology, National Institute of Sensory Organs, Tokyo, Japan.

[2] Department of Ophthalmology, National Tokyo Medical Center, Tokyo, Japan.

[3] Akiba Eye Clinic, Niigata, Japan.

Financial Disclosure(s):
The author(s) have no proprietary or commercial interest in any materials discussed in this article.

Supported in part by research grants from the Ministry of Health, Labor and Welfare, Tokyo, Japan; and the Japan Science and Technology Agency, Tokyo, Japan.

Correspondence:
Kazushige Tsunoda, Laboratory of Visual Physiology, National Institute of Sensory Organs, 2-5-1 Higashigaoka, Meguro-ku, Tokyo 152-8902, Japan.
E-mail: tsunodakazushige@kankakuki.go.jp.

lone for the study. Allergan, Inc has provided unrestricted funds to DRCR.net for its discretionary use.

Role of the Sponsor: The funding organization participated in oversight of the conduct of the study and review of the manuscript but not directly in the design of the study, the conduct of the study, data collection, data management, data analysis, interpretation of the data, or preparation of the manuscript. As per the DRCR.net Industry Collaboration Guidelines (http://www.drcr.net), DRCR.net had complete control over the design of the protocol, ownership of the data, and all editorial content of presentations and publications related to the protocol.

1. Diabetic Retinopathy Clinical Research Network. A randomized trial comparing intravitreal triamcinolone acetonide and focal/grid photocoagulation for diabetic macular edema. *Ophthalmology* 2008;115(9):1447-1449, 1449, e1-e10
2. Bakri SJ, Pulido JS, McCannel CA, Hodge DO, Diehl N, Hillemeier J. Immediate intraocular pressure changes following intravitreal injections of triamcinolone, pegaptanib, and bevacizumab. *Eye (Lond)*. 2009;23(1):181-185
3. Benz MS, Albini TA, Holz ER, et al. Short-term course of intraocular pressure after intravitreal injection of triamcinolone acetonide. *Ophthalmology* 2006; 113(7):1174-1178
4. Jonas JB, Degenring RF, Kreissig I, Akkoyun I, Kamppeter BA. Intraocular pressure elevation after intravitreal triamcinolone acetonide injection. *Ophthalmology* 2005;112(4):593-598
5. Clark AF, Wordinger RJ. The role of steroids in outflow resistance. *Exp Eye Res* 2009;88(4):752-759
6. Clark AF, Morrison JC. Steroid-induced glaucoma. In: Morrison JC, Pollack IP, eds. *Glaucoma. Science and Practice*. New York, NY: Thieme; 2003

Selective Abnormality of Cone Outer Segment Tip Line in Acute Zonal Occult Outer Retinopathy as Observed by Spectral-Domain Optical Coherence Tomography

Optical coherence tomography (OCT) plays an important role in the diagnosis of retinal diseases with minimal ophthalmoscopic changes. For example, in eyes with acute zonal occult outer retinopathy (AZOOR),[1-5] an abnormality of the photoreceptor inner segment–outer segment (IS/OS) junction found by OCT was spatially correlated with the region of visual field defect. Recent high-resolution spectral-domain OCT images have shown a thin line between the IS/OS junction and the retinal pigment epithelium. This line has been identified as the cone OS tip (COST) line.[6] However, the pathophysiological interpretation of its appearance has not been established, and the diagnostic value of the COST line has yet to be determined.

We report 2 cases of AZOOR, both of which showed acute central scotoma with an enlarged blind spot. The ophthalmoscopic and angiographic changes were minimal, but electroretinography (ERG) revealed reduced responses in the affected regions. In both cases, the IS/OS junction on the OCT image was normal, but the COST line was not present or appeared indistinct in the region of visual field defect. Our findings suggest that the COST line may be an early indicator of cone photoreceptor dysfunction in eyes with minimal ophthalmoscopic abnormalities.

Report of Cases. Patient 1 (a 24-year-old woman) and patient 2 (a 28-year-old woman) both had sudden unilateral visual disturbances following photopsia. The visual acuities were 0.02 OD and 1.5 OS in patient 1 and 0.15 OD and 1.5 OS in patient 2. Goldmann kinetic perimetry revealed a blind spot enlargement and central scotoma in the right eye of both patients (**Figure 1** and **Figure 2**). The anterior segment and fundus were normal; however, fluorescein angiography showed a slightly mottled hyperfluorescence around the macula in the affected eye of both patients. The full-field scotopic ERGs were normal, but there were phase delays in the photopic 30-Hz ERGs in the affected eyes: 5.7 milliseconds in patient 1 and 8.0 milliseconds in patient 2. In addition, the amplitudes of the photopic b-waves were reduced in both patients. The focal macular ERGs (ER80; Kowa Co, Tokyo, Japan, and Mayo Co, Nagoya, Japan) in the central 15° were almost flat in the affected eye in both patients. Neither patient had systemic disorders such as viral infections or autoimmune diseases.

Spectral-domain OCT (Carl Zeiss Meditec, Dublin, California) showed the IS/OS junction clearly, even in the region of the scotoma. However, the COST line was not detected in patient 1 and appeared indistinct in patient 2 (Figure 1 andFigure 2). Moreover, the bulgelike structure of the IS/OS junction at the fovea (with the foveal bulge indicating a domelike appearance of the IS/OS junction due to an elongated cone OS at the fovea)[7] could not be observed in the affected eyes. The visual disturbances of these patients did not recover, and these abnormalities in the OCT images were observed at all examinations for 50 months in patient 1 and 18 months in patient 2 after the onset.

Comment. To our knowledge, this is the first report of AZOOR where the boundary of the IS/OS junction in the OCT images was well preserved but the COST line was absent or indistinct from the initial examination through the entire follow-up period. Earlier studies demonstrated that a loss or irregularity of the IS/OS junction observed by OCT corresponded well with the visual field defects even at the early stages of AZOOR,[2-5] and the abnormality in the IS/OS junction can improve following recovery of the scotoma. These findings have led to the hypothesis that photoreceptor OS dysfunction is the primary lesion in AZOOR.

The COST line corresponds to the junction between the photoreceptor tips and the apical processes of the retinal pigment epithelium, where photoreceptor OS disc membranes are continuously shed for renewal.[6] Thus, the appearance of the COST line may reflect the normal function of the photoreceptor OSs more closely than the IS/OS junction. In fact, in all of the AZOOR cases we have recently examined, the COST line was always absent in the region of IS/OS abnormalities, suggesting that the abnormality of the COST line may precede that of the IS/OS junction. In our 2 cases, the fundus appeared normal and the IS/OS junction was clearly observed in the region of the COST line abnormality for 50 and 18 months after the onset. The focal macular ERGs, however, were markedly reduced in the affected areas. In the OCT images, the cone photoreceptor dysfunction corresponding to the region of scotoma could be detected only by the abnormality of the COST line.

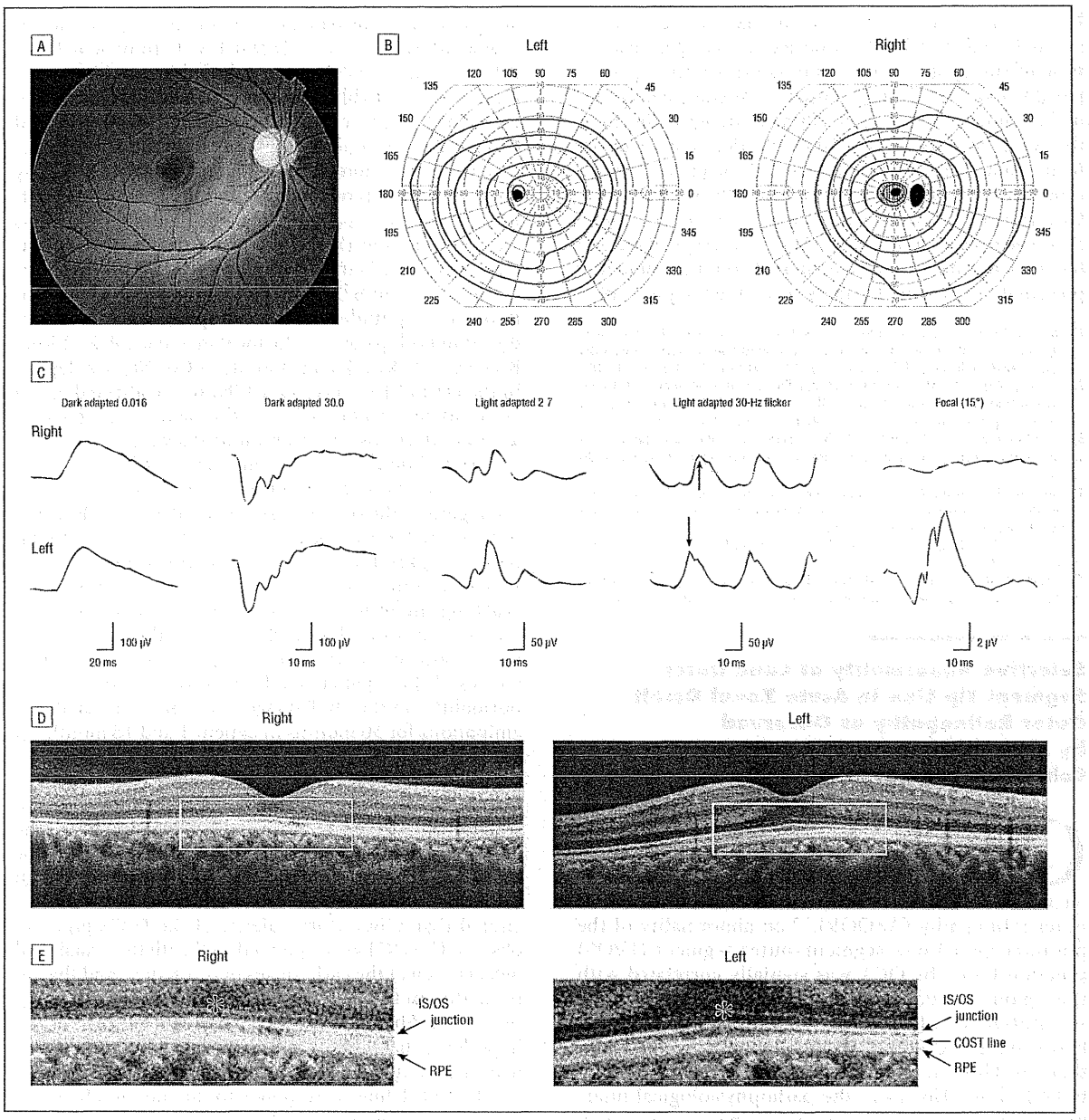

Figure 1. Findings in patient 1. A, Fundus photograph of the right eye showing a normal appearance. B, Goldmann kinetic perimetry showing a blind spot enlargement and central scotoma in the right eye. C, Full-field and focal macular electroretinograms. The latencies of the photopic 30-Hz flicker responses are delayed in the right eye. Arrows indicate the phase difference in light-adapted 30-Hz flicker responses. The focal macular electroretinogram is almost flat in the central 15° of the right eye. Optical coherence tomographic images vertically profiled along the foveola (D) and magnified optical coherence tomographic images in the region of visual field abnormality (E). In the left eye, the inner segment–outer segment (IS/OS) junction, foveal bulge, and cone OS tip (COST) line are clearly observed. In the right eye, the IS/OS junction is clearly observed but the COST line is absent in the macula. The foveal bulge (asterisk) cannot be observed in the right eye. RPE indicates retinal pigment epithelium.

Our findings suggest that the dysfunction of the cone photoreceptor OS could be initially reflected by an absence or indistinctness of the COST line and the absence of the foveal bulge.[5] These changes may be followed by the development of abnormalities in the IS/OS junction in the more advanced stages. However, in our cases, the IS/OS junction remained the same during the entire follow-up period. This may suggest another possibility that our 2 cases constitute a subtype of AZOOR. However, in another case of AZOOR with a blind spot enlargement and relative central scotoma (a 21-year-old woman, data not shown), both the IS/OS and COST lines disappeared in the peripapillary region where visual field disturbance was severe, whereas only the COST line disappeared and the IS/OS line remained normal in the foveal region where the visual field disturbance was milder. These findings support the idea that the visibility of the COST line is more easily affected than that of

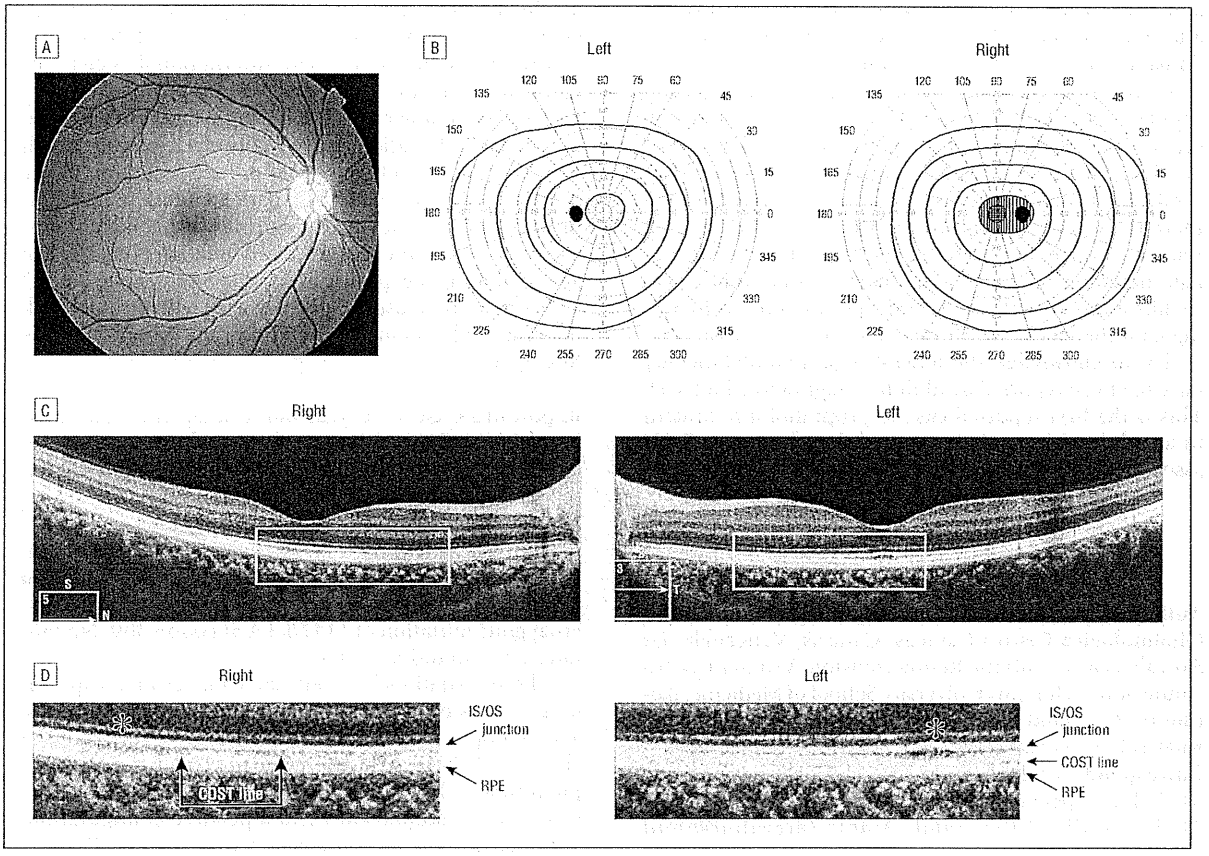

Figure 2. Findings in patient 2. A, Fundus photograph of the right eye showing a normal appearance. B, Goldmann kinetic perimetry showing a blind spot enlargement and central scotoma in the right eye. Optical coherence tomographic images horizontally profiled along the foveola (C), and magnified optical coherence tomographic images in the region of the visual field abnormality (D). In both eyes, the inner segment–outer segment (IS/OS) junction is clearly observed. In the right eye, the cone OS tip (COST) line is partially observed but appeared more indistinct than in the left eye. The foveal bulge (asterisk) cannot be seen in the right eye.

the IS/OS line at an earlier stage by the pathological changes in a typical case of AZOOR. We should note that care should be taken in evaluation of the COST line because its visibility is dependent on the intensity and direction of the laser light that reaches the photoreceptor layer.[6] However, in patients with AZOOR, the COST line and the foveal bulge observed by OCT could help as indicators of early cone photoreceptor dysfunction in cases with minimal ophthalmoscopic and angiographic abnormalities.

Kazushige Tsunoda, MD
Kaoru Fujinami, MD
Yozo Miyake, MD

Author Affiliations: National Institute of Sensory Organs, Tokyo (Drs Tsunoda and Fujinami), and Aichi Medical University, Aichi (Dr Miyake), Japan.
Correspondence: Dr Tsunoda, Laboratory of Visual Physiology, National Institute of Sensory Organs, 2-5-1 Higashigaoka, Meguroku, Tokyo 1528902, Japan (tsunodakazushige@kankakuki.go.jp).
Financial Disclosure: None reported.
Funding/Support: This work was supported by research grants from the Ministry of Health, Labor, and Welfare, Japan, and by SENTAN, Japan Science and Technology Agency, Japan.

1. Gass JD, Agarwal A, Scott IU. Acute zonal occult outer retinopathy: a long-term follow-up study. *Am J Ophthalmol*. 2002;134(3):329-339.
2. Li D, Kishi S. Loss of photoreceptor outer segment in acute zonal occult outer retinopathy. *Arch Ophthalmol*. 2007;125(9):1194-1200.
3. Zibrandtsen N, Munch IC, Klemp K, Jørgensen TM, Sander B, Larsen M. Photoreceptor atrophy in acute zonal occult outer retinopathy. *Acta Ophthalmol*. 2008;86(8):913-916.
4. Spaide RF, Koizumi H, Freund KB. Photoreceptor outer segment abnormalities as a cause of blind spot enlargement in acute zonal occult outer retinopathy-complex diseases. *Am J Ophthalmol*. 2008;146(1):111-120.
5. Takai Y, Ishiko S, Kagokawa H, Fukui K, Takahashi A, Yoshida A. Morphological study of acute zonal occult outer retinopathy (AZOOR) by multiplanar optical coherence tomography. *Acta Ophthalmol*. 2009;87(4):408-418.
6. Srinivasan VJ, Monson BK, Wojtkowski M, et al. Characterization of outer retinal morphology with high-speed, ultrahigh-resolution optical coherence tomography. *Invest Ophthalmol Vis Sci*. 2008;49(4):1571-1579.
7. Curcio CA, Sloan KR, Kalina RE, Hendrickson AE. Human photoreceptor topography. *J Comp Neurol*. 1990;292(4):497-523.

Adult Ovarian Retinoblastoma Genomic Profile Distinct From Prior Childhood Eye Tumor

We report the first case of a woman, previously cured of childhood intraocular retinoblastoma, who developed tumor in the ovary with histological and genomic characteristics suggesting an independent retinoblastoma, not a metastasis.

addition, the duration of treatment to induce retinal reattachment is currently unknown. However, patients with IH have been treated for several months.

Hemangiomas consist histologically of cavernous and capillary vascular networks. The mechanism by which oral propranolol aids in the resolution of exudative retinal detachment in DCH associated with Sturge-Weber syndrome is unknown. It is possible that, similar to IH, there is vasoconstriction of the DCH due to decreased release of nitric oxide, blocking of proangiogenic signals including vascular endothelial growth factor and basic fibroblast growth factor, and apoptosis in proliferating endothelial cells with vascular tumor regression.[5]

To our knowledge, the benefits of propranolol therapy have not been reported in adult hemangioma or for DCH. This is the first reported case of propranolol treatment in an adult with exudative retinal detachment in DCH associated with Sturge-Weber syndrome.

J. Fernando Arevalo, MD
Juan D. Arias, MD
Martin A. Serrano, MD

Author Affiliations: Retina and Vitreous Service, Clínica Oftalmológica Centro Caracas, Caracas, Venezuela. Dr Arevalo is now with the Retina Division, Wilmer Eye Institute, Johns Hopkins University School of Medicine, Baltimore, Maryland, and the Vitreoretinal Division, King Khaled Eye Specialist Hospital, Riyadh, Saudi Arabia.
Correspondence: Dr Arevalo, Vitreoretinal Division, King Khaled Eye Specialist Hospital, Al-Oruba Street, PO Box 7191, Riyadh 11462, Saudi Arabia (arevalojf@jhmi.edu).
Financial Disclosure: None reported.
Funding/Support: This work was supported in part by the Arevalo-Coutinho Foundation for Research in Ophthalmology, Caracas, Venezuela.
Previous Presentation: This paper was presented at the 34th Annual Meeting of the Macula Society; March 9, 2011; Boca Raton, Florida.

1 Schilling H, Sauerwein W, Lommatzsch A, et al Long-term results after low dose ocular irradiation for choroidal haemangiomas. *Br J Ophthalmol.* 1997; 81(4).267-273.
2. Anand R. Photodynamic therapy for diffuse choroidal hemangioma associated with Sturge Weber syndrome. *Am J Ophthalmol.* 2003,136(4)·758-760.
3 Léauté-Labrèze C, Dumas de la Roque E, Hubiche T, Boralevi F, Thambo JB, Taïeb A Propranolol for severe hemangiomas of infancy *N Engl J Med.* 2008; 358(24)·2649-2651
4 Siegfried EC, Keenan WJ, Al-Jureidini S More on propranolol for hemangiomas of infancy. *N Engl J Med.* 2008;359(26) 2846.
5 Storch CH, Hoeger PH. Propranolol for infantile haemangiomas· insights into the molecular mechanisms of action. *Br J Dermatol.* 2010,163(2):269-274.
6 Sans V, de la Roque ED, Berge J, et al. Propranolol for severe infantile hemangiomas· follow-up report. *Pediatrics.* 2009;124(3).e423-e431.

Oguchi Disease With Unusual Findings Associated With a Heterozygous Mutation in the *SAG* Gene

Oguchi disease is a type of congenital stationary night blindness with an autosomal recessive inheritance pattern. Two causative genes have been reported for Oguchi disease: the *SAG* and *GRK1* genes. Homozygous Oguchi disease is characterized by a golden-yellow discoloration of the fundus that disappears after prolonged dark adaptation, called the Mizuo-Nakamura phenomenon. The International Society for Clinical Electrophysiology of Vision–protocol bright-flash electroretinograms (ERGs), performed after 30 minutes of dark adaptation, are typically electronegative with a severely reduced b-wave and milder reduction of the a-wave.[1,2] After 3 to 4 hours of dark adaptation, both amplitudes recover to nearly normal, especially the a-wave.[2] However, the recovered rod function is rapidly lost after a short light exposure or a single bright white flash.[2,3]

We describe a case of Oguchi disease with unusual findings caused by a putative heterozygous mutation in the *SAG* gene.

Report of a Case. A 40-year-old woman with visual acuity of 20/20 OU had fundus abnormalities and was referred to our institute. She had photophobia but did not report night blindness. There was no autosomal dominant family history. The retina had a golden-yellow appearance (**Figure**, A). The Mizuo-Nakamura phenomenon was observed after 30 minutes of dark adaptation (Figure, B). Sequencing of the *SAG* gene identified a heterozygous mutation of 1147del A at codon 309. No mutation was found in *GRK1*.

The International Society for Clinical Electrophysiology of Vision protocol was used to record the ERGs. The scotopic ERGs after 30 minutes of dark adaptation showed slightly reduced amplitude and delayed implicit time in b-wave (Figure, C). The bright-flash ERG (30 candelas·seconds/m^2) had a positive configuration, although the b:a ratio was lower than normal (Figure, C). The photopic and flicker ERGs performed after 10 minutes of light adaptation were normal (Figure, C). To determine the extent of the rod function recovery, bright-flash ERGs were recorded 4 times at 30-second intervals after 30 minutes of dark adaptation. During the 4 stimuli, the waveform changed from the positive pattern to a negative configuration with a severely reduced b-wave and additional milder reduction of the a-wave, which is characteristic of homozygous Oguchi disease (Figure, D). To our knowledge, this phenomenon has never been reported in normal eyes, in eyes with the typical type of Oguchi disease, or in other cases of Oguchi disease with the same heterozygous *SAG* mutation (Figure, D). The superimposed ERGs elicited by the 4 consecutive flashes show the variation of rod function recovery (Figure, E).

Comment. To our knowledge, this is the first case of Oguchi disease with a distinct fundus appearance and mild electrophysiological abnormalities associated with a putative heterozygous *SAG* mutation. However, we cannot exclude the possibility that another mutation exists in the intron of another allele, which causes the mild phenotype in this patient.

The repetitive-flash ERG protocol was crucial for the diagnosis. It has been reported that double- or triple-flash stimulations after prolonged dark adaption induce ERG alterations in typical patients with Oguchi disease.[3] However, the use of a 30-second interval allowed us to follow the degree of rod function recovery.

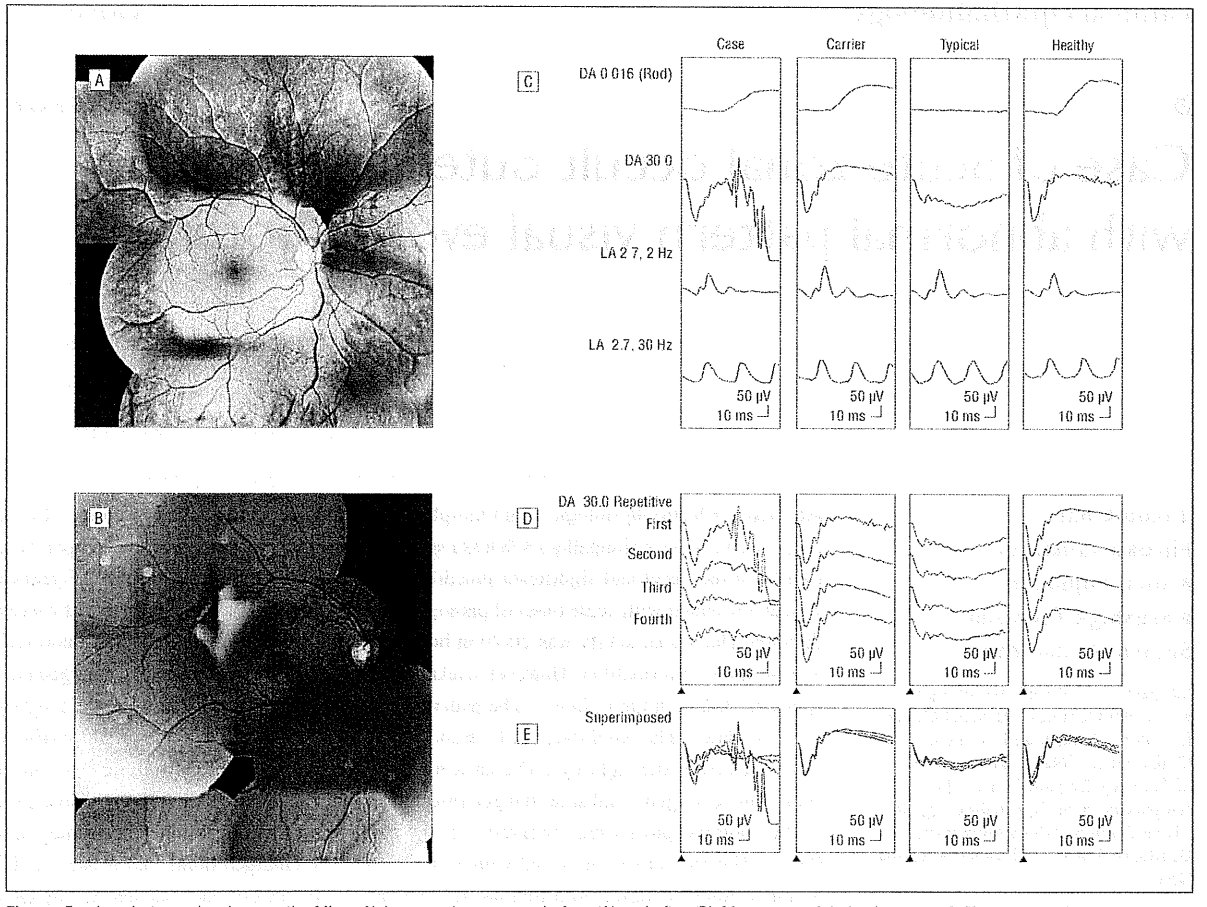

Figure. Fundus photographs showing the Mizuo-Nakamura phenomenon before (A) and after (B) 30 minutes of dark adaptation. C, The electroretinograms (ERGs) recorded according to the International Society for Clinical Electrophysiology of Vision protocol. D, The ERGs elicited by 4 repetitive flashes at interstimulus intervals of 30 seconds. E, Superimposed ERGs elicited by 4 flashes. The ERGs are from our patient with Oguchi disease (case), another patient with Oguchi disease with a heterozygous mutation (carrier), a typical patient with Oguchi disease, and a healthy subject. DA indicates dark adaptation, LA, light adaptation.

Arrestin and rhodopsin kinase act in sequence to deactivate rhodopsin to stop the phototransduction cascade.[4] Results of molecular biological studies have suggested that residual arrestin activity correlates with the severity of the clinical phenotype.[5] However, in our case it was more difficult to determine the relationship between the putative heterozygous mutation of the *SAG* gene and the mild electrophysiological abnormalities in the rod function recovery. A modifying effect of deactivating rhodopsin should be considered.

The time required for the reappearance of the rod function demonstrated in the electrophysiological study and the time required to demonstrate the Mizuo-Nakamura phenomenon were nearly identical. We suggest that the physiological basis for the Mizuo-Nakamura phenomenon may be closely related to the abnormal deactivation of rhodopsin.

Kaoru Fujinami, MD
Kazushige Tsunoda, MD, PhD
Makoto Nakamura, MD, PhD
Yoshihisa Oguchi, MD, PhD
Yozo Miyake, MD, PhD

Author Affiliations: Laboratory of Visual Physiology, National Institute of Sensory Organs, National Tokyo Medical Center (Drs Fujinami, Tsunoda, and Miyake) and Department of Ophthalmology, Keio University of Medicine (Dr Oguchi), Tokyo, and Department of Ophthalmology, Nagoya University Graduate School of Medicine, Aichi (Dr Nakamura), Japan.

Correspondence: Dr Tsunoda, Laboratory of Visual Physiology, National Institute of Sensory Organs, National Tokyo Medical Center, 2-5-1, Higashigaoka, Meguro-ku, Tokyo 152-8902, Japan (tsunodakazushige@kankakuki.go.jp).

Financial Disclosure: None reported.

1. Carr RE, Gouras P. Oguchi's disease. *Arch Ophthalmol*. 1965;73:646-656.
2. Miyake Y, Horiguchi M, Suzuki S, Kondo M, Tanikawa A. Electrophysiological findings in patients with Oguchi's disease. *Jpn J Ophthalmol*. 1996;40(4):511-519.
3. Gouras P. Electroretinography: some basic principles. *Invest Ophthalmol*. 1970;9(8):557-569.
4. Ohguro H, Van Hooser JP, Milam AH, Palczewski K. Rhodopsin phosphorylation and dephosphorylation in vivo. *J Biol Chem*. 1995;270(24):14259-14262.
5. Dryja TP. Molecular genetics of Oguchi disease, fundus albipunctatus, and other forms of stationary night blindness: LVII Edward Jackson Memorial Lecture. *Am J Ophthalmol*. 2000;130(5):547-563.

Clinical Ophthalmology

Dovepress

open access to scientific and medical research

Open Access Full Text Article

CASE REPORT

Case of acute zonal occult outer retinopathy with abnormal pattern visual evoked potentials

Yuzhu Chai[1]
Hiroko Yamazaki[1]
Kaoru Fujinami[2]
Kazushige Tsunoda[2]
Shuichi Yamamoto[3]

[1]Department of Ophthalmology, Kohnodai Hospital, National Center for Global Health and Medicine, Chiba, Japan; [2]National Institute of Sensory Organs, Tokyo, Japan; [3]Department of Ophthalmology and Visual Science, Chiba University Graduate School of Medicine, Chiba, Japan

Abstract: Electrophysiological and morphological findings were studied in a case of acute zonal occult outer retinopathy (AZOOR) showing abnormal pattern visual evoked potentials (VEPs) at the onset and significant functional recovery in the natural course. A 21-year-old woman presented with acute onset of photopsia and a large scotoma in the right eye of 2 weeks duration. Her visual acuity was 20/20 in both eyes with no ophthalmoscopic and fluorescein angiographic abnormalities. However, a relative afferent pupillary defect and an enlarged blind spot were found in the right eye. The pattern VEPs were severely reduced when the right eye was stimulated. The amplitudes of both rod and cone full-field electroretinographics (ERGs) were reduced in the right eye. The amplitudes of the multifocal ERGs were reduced in the area of the enlarged blind spot. Irregularities in the inner segment/outer segment (IS/OS) line of the photoreceptors were observed over the nasal fovea by optical coherence tomography (OCT). The patient was followed without treatment. The enlarged blind spot disappeared in 3 months after the onset. At 5 months, reappearance of the IS/OS line was detected by OCT. At 6 months, the P_{100} recovered to normal values. At 1 year, the reduced full-field ERGs were almost normal size and the multifocal ERGs in the area corresponding to the enlarged blind spot were also improved. ERG findings are crucial for differentiating AZOOR from retrobulbar neuritis, especially in patients with abnormal pattern VEPs. The pattern VEPs, full-field ERGs, multifocal ERGs, and OCT images can be abnormal in the early phase of AZOOR, but they can all improve during the natural course.

Keywords: AZOOR, pattern VEP, full-field ERG, multifocal ERG, OCT

Introduction

Acute zonal occult outer retinopathy (AZOOR), first reported in 1993 by Gass,[1] is characterized by an acute onset of photopsia, scotoma, minimal funduscopic changes, and electroretinographic (ERG) abnormalities affecting one or both eyes. The presence of abnormal ERGs is important for the diagnosis of AZOOR, and the ERG findings suggest a dysfunction of the photoreceptors.[1–5] Recent optical coherence tomographic (OCT) studies have shown morphological alterations of the photoreceptors.[6–9]

Although a viral or autoimmune etiology has been suspected, no cause is readily identifiable in this group of generally healthy patients. Some patients with AZOOR have been misdiagnosed with optic nerve disorders because they had an afferent pupillary defect, a scotoma, and no obvious fundus abnormalities.[1–3]

It has been reported that the natural course of AZOOR is varied,[1–3] although there is still no known treatment. There are few detailed reports about AZOOR patients who showed subjective and objective improvements in their visual function.

Correspondence: Yuzhu Chai
Department of Ophthalmology, Kohnodai Hospital, National Center for Global Health and Medicine,
1-7-1 Kohnodai Ichikawa City,
Chiba 2728516, Japan
Tel +81 47 372 3501
Fax +81 47 372 1858
Email chai_yuzhujp@yahoo.co.jp

We report a case of AZOOR, showing abnormal pattern visual evoked potentials (VEPs) at the onset and significant functional recovery in the natural course.

Case report

A healthy 21-year-old woman reported that she had a sudden onset of photopsia and a large scotoma in the right eye on August 14, 2008. She visited her ophthalmologist on August 15, and the initial examination showed no abnormalities of the fundus in both eyes but a large scotoma was detected by static perimetry in the right eye. She was referred to us for further examination on August 29. She reported that she had no systemic problems and was not taking any medications. Her best-corrected visual acuity was 20/20 bilaterally, and the refractive error was −9.5 diopters in the right eye and −8.5 diopters in the left eye. However, she had a relatively afferent pupillary defect in the right eye. The results of ophthalmoscopy (Figure 1A), fluorescein angiography (Figure 1B), blood screening, and brain magnetic resonance imaging (MRI) were within normal limits. Static perimetry with the Humphrey field analyzer showed an enlarged blind spot in the right eye (Figure 1C). The pattern VEPs elicited by transient and steady-state stimuli to the right eye were severely reduced (Figure 2). She was suspected of having retrobulbar neuritis at this point of time. VEPs were recorded by Nihon Kohden MEB-2200 Neuropack (Tokyo, Japan) with the active electrode placed at Oz. The reference electrode was located at the right earlobe and the ground electrode at the left earlobe. The visual stimulus was a black and white check board pattern generated on a television monitor. The check size was 20 minutes of arc. The contrast was 80%, and the mean luminance was kept at 50 cd/m^2. The stimulus field of the pattern was 7 × 11 degrees. The pattern was reversed at three reversals per second for transient VEP, and 10 reversals per second for steady-state VEP. The electrodes were connected to a preamplifier with a bandpass of 1 to 100 Hz, and for each measurement, 100 responses were averaged. The patient fixed on a point in the center of the pattern monocularly from an observing distance of 170 cm, with an undilated pupil under full refractive correction.

To eliminate the possibility that the patient had AZOOR, full-field ERGs and multifocal ERGs were recorded. The amplitudes of the rod and cone responses in the right eye were reduced to about 50% of those in

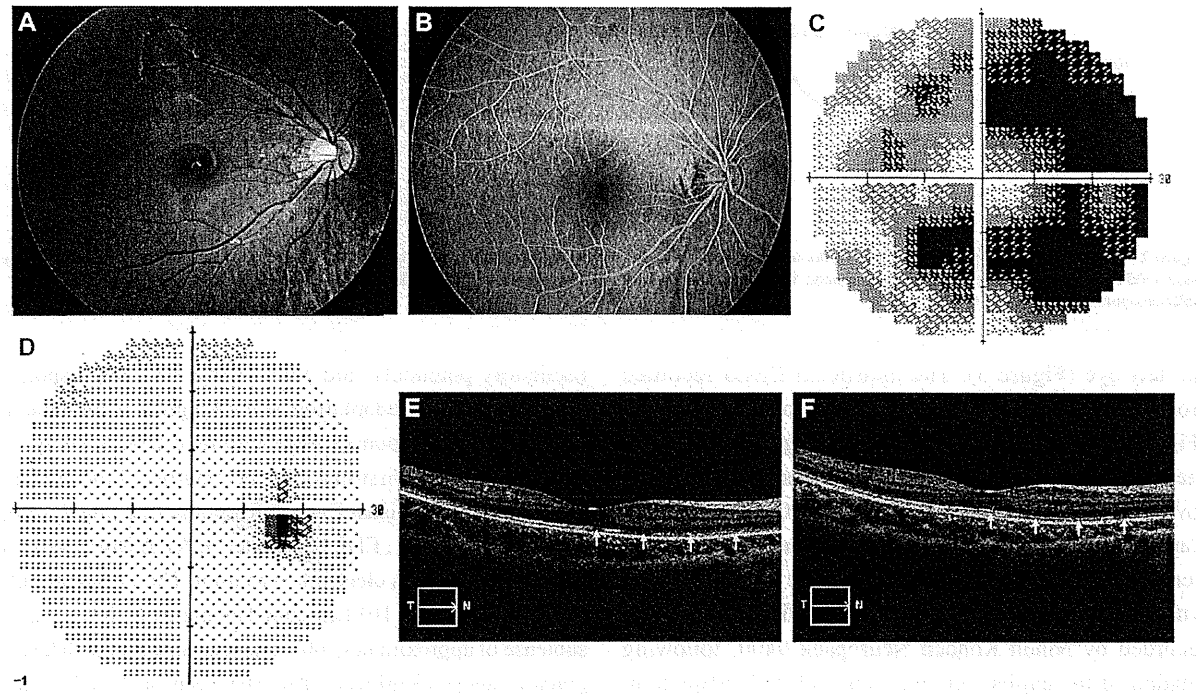

Figure 1 Fundus photograph, fluorescein angiographic image, Humphrey static perimetry, and Optical coherence tomography (OCT) of the right eye. (A) Fundus photograph at the onset showing that the retina was normal. (B) Fluorescein angiography at the onset showing normal vascular pattern and no leakage. (C) Humphrey static perimetry at the onset showing enlarged blind spot (30-2 strategy MD −21.97 dB). (D) Humphrey static perimetry 3 months after the onset showing marginally enlarged blind spot (30-2 strategy MD −1.90 dB). (E) OCT image at the onset showing irregular inner segment/outer segment (IS/OS) line over the nasal fovea. (F) OCT image 5 months after the onset showing reappearance of IS/OS line over the nasal fovea.

Abbreviation: MD, mean defect.

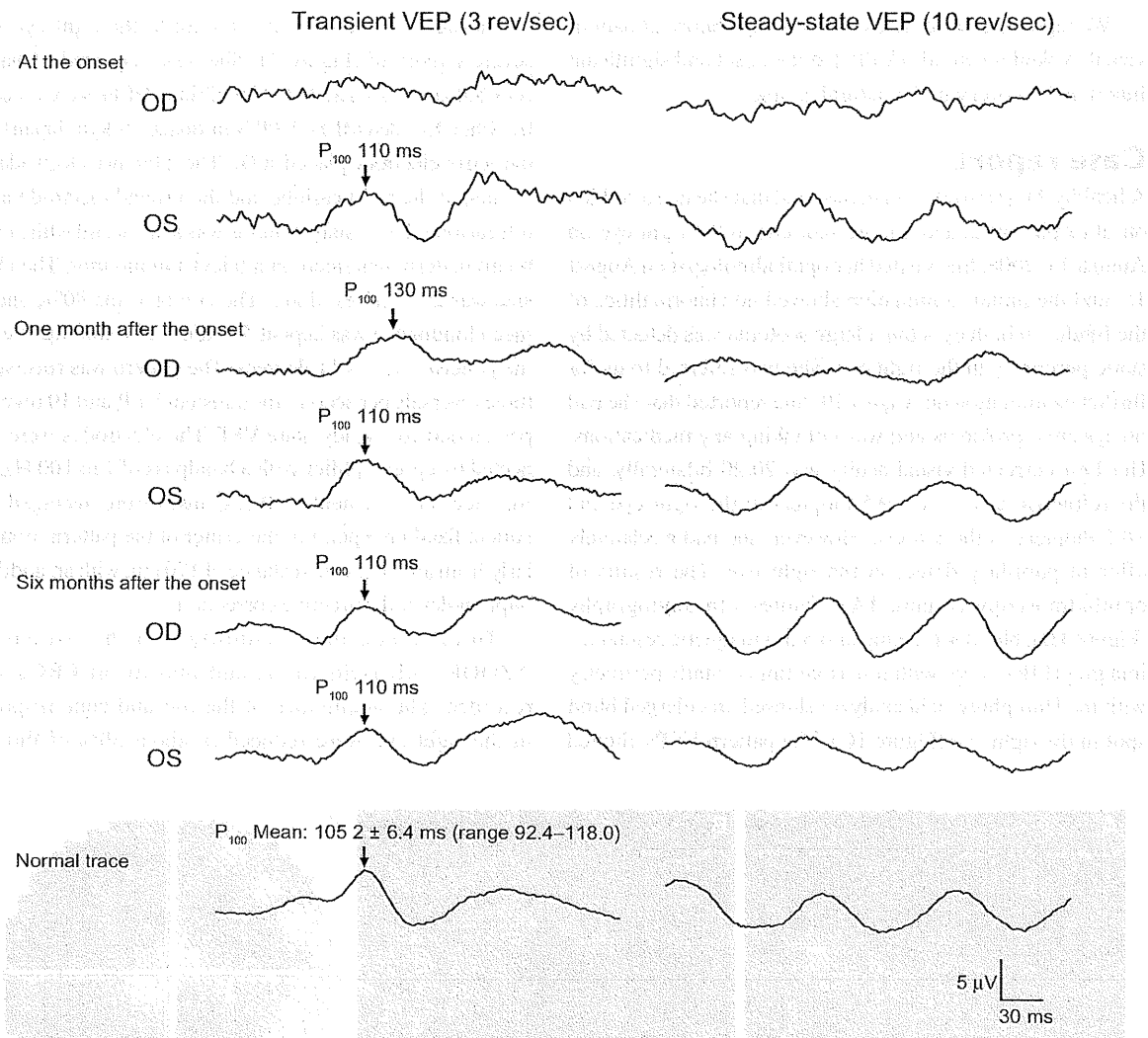

Figure 2 Pattern visual evoked potentials (VEPs). At the onset, pattern VEPs are severely reduced in the right eye. One month after the onset, the P_{100} component of the pattern VEPs has a prolonged latency of 130 milliseconds. Six months after the onset, the P_{100} recovers to 110 milliseconds.
Abbreviations: OD, right eye; OS, left eye.

the left eye (Figure 3). The multifocal ERGs recorded from the area of the enlarged blind spot were reduced (Figure 4). Irregularities in the inner segment/outer segment (IS/OS) line of the photoreceptors over the nasal fovea were observed by Fourier-domain OCT (HD-OCT; Carl Zeiss Meditec, Oberkochen, Germany) (Figure 1E). Serum anti-recoverin was negative. She was diagnosed with AZOOR from these findings. Full-field ERGs were recorded by Nihon Kohden Neuropack 9400, following dilation of the pupils and 30 minutes of dark adaptation. A contact lens electrode was used. The reference electrode was placed at the forehead and the ground electrode at the earlobe. The flash strength was 0.01 cd s m^{-2} for rod response, 80.0 cd s m^{-2} for combined rod–cone response and oscillatory potentials, and 3.0 cd s m^{-2} for cone response and flicker. Light adaptation and background luminance was 25 cd/m^2. Responses were amplified with a bandpass of 0.2 to 1000 Hz. First-order Kernel multifocal ERGs were recorded with the Visual Evoked Response Imaging System (VERIS science 4.1; EDI, San Mateo, CA). A Burian-Allen bipolar contact lens electrode was used. The visual stimuli consisted of 61 and 103 hexagonal elements with an overall subtense of approximately 60°. The luminance of each hexagon was independently modulated between black (3.5 cd/m^2) and white (138.0 cd/m^2) according to a binary M-sequence at 75 Hz. The surround luminance was 70.8 cd/m^2.

The patient was followed without any treatment, and more comprehensive examinations were made in her follow-up

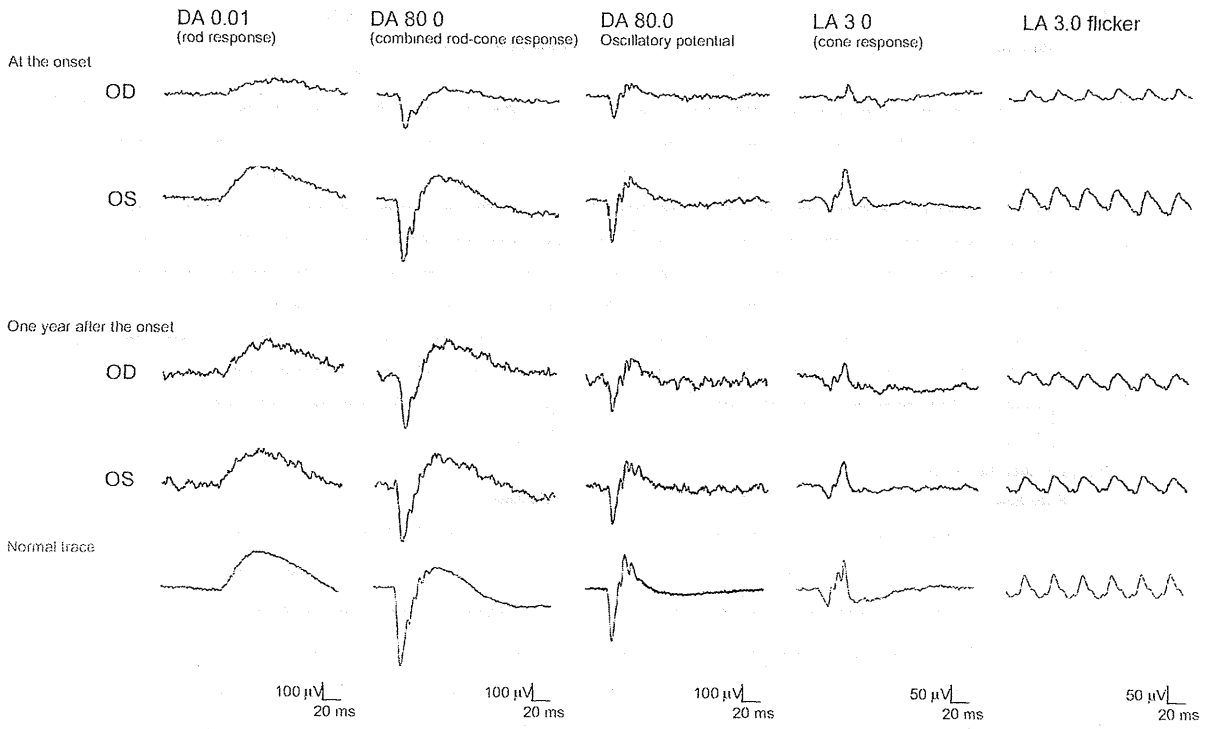

Figure 3 Full-field electroretinographics (ERGs). At the onset, the amplitudes of the rod and cone responses in the right eye are reduced to about 50% of those in the left eye. At the 1 year follow-up examination, the reduced full-field ERGs are improved to be approximately the same amplitudes as those from the left eye.
Abbreviations: DA, dark adapted; LA, light adapted; OD, right eye; OS, left eye.

examinations. The enlarged blind spot in static perimetry disappeared 3 months after our initial examination (Figure 1D). The P_{100} component of the pattern VEPs had a prolonged latency of 130 milliseconds 1 month later. At 6 months, the P_{100} recovered to 110 milliseconds (mean: 105.2 ± 6.4 milliseconds; normal range: 92.4–118.0 milliseconds) (Figure 2). At 5 months, reappearance of the IS/OS line was detected by OCT over the nasal fovea (Figure 1F). At the 1 year follow-up examination, her best-corrected visual acuity was 20/20 in both eyes. The reduced full-field ERGs were improved to be approximately the same amplitudes as those from the left eye (Figure 3). A mild improvement of the reduced multifocal ERGs was also observed (Figure 4). The other findings had not worsened.

Discussion

In 1993, Gass introduced AZOOR to describe a previously unrecognized syndrome occurring predominantly in young females. In his original series of 13 patients, affected individuals typically presented with acute onset of photopsia, scotoma, minimal funduscopic changes, and ERG abnormalities affecting one or both eyes.[1] The presence of abnormal ERGs is essential for the diagnosis of AZOOR. Gass et al reported that electroretinographic amplitudes were depressed in all 90 affected eyes.[2] Jacobson et al reported 24 patients with AZOOR showing abnormal ERGs. Interocular asymmetry was a prominent feature.[4] Francis et al reported that electrophysiology demonstrated a consistent pattern of dysfunction both at the photoreceptor/retinal pigment epithelial complex but also at inner retinal levels in 28 patients with AZOOR.[5]

Our case presented with a sudden onset of photopsia and a large scotoma in the right eye at the onset. The normal fundus, large scotoma, and the afferent pupillary defect made us suspect retrobulbar neuritis at first. But the absence of retrobulbar pain at rest or on eye movement, which is a common symptom in retrobulbar neuritis,[10] and the presence of photopsia, which is a typical symptom of AZOOR,[1–5] made us suspect AZOOR at the same time. Further examinations were taken to make a definite diagnosis.

Our patient had an extinguished P_{100} component of the pattern VEPs at the onset, although her visual acuity was 20/20. Fluorescein angiography showed normal vascular pattern and no leakage. MRI showed no changes in the optic nerve. Strikingly, in full-field ERGs, the amplitudes of both rod and cone responses were reduced in the right eye. The amplitudes of the multifocal ERGs were reduced in the area

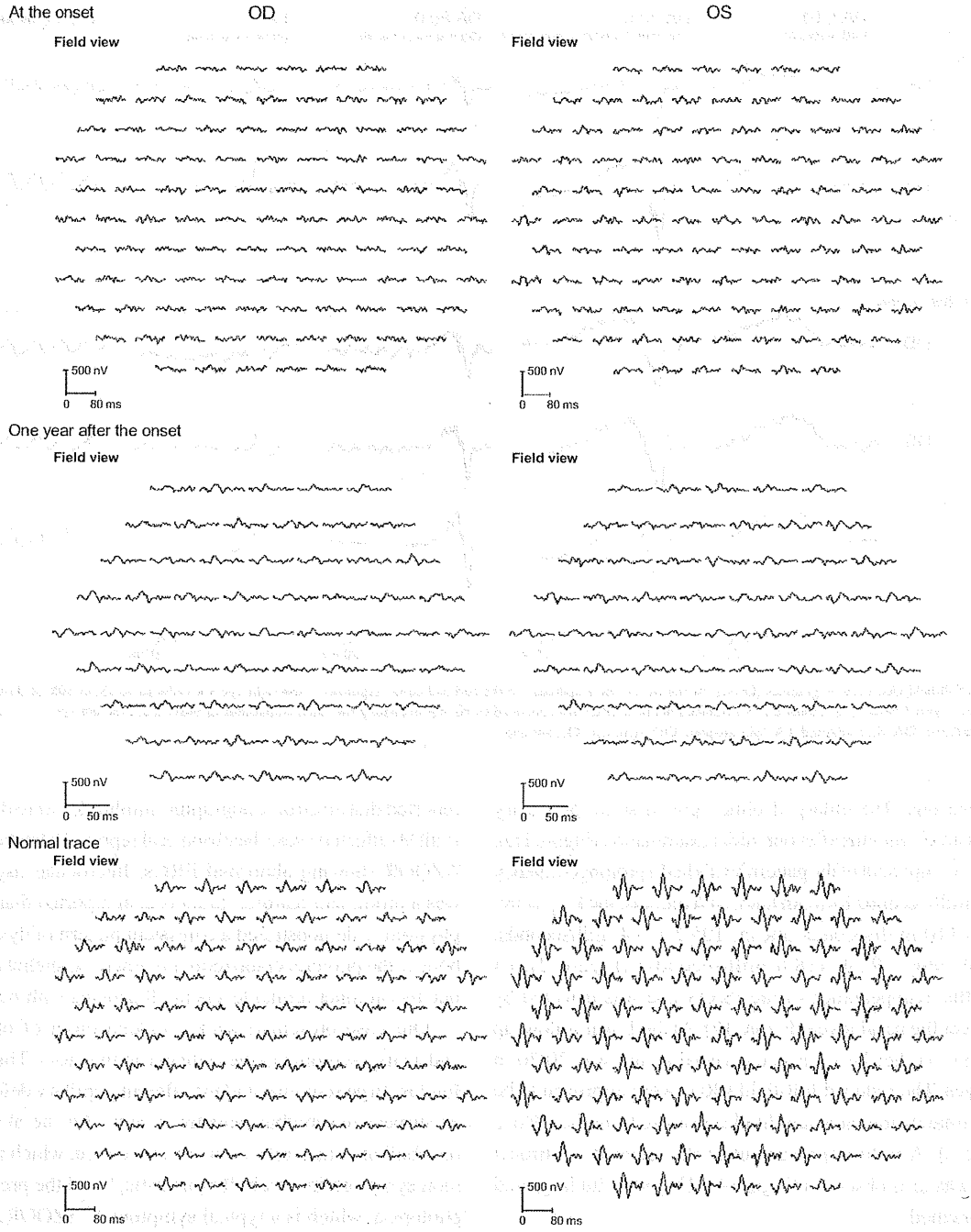

Figure 4 Multifocal electroretinographics (ERGs). At the onset, the multifocal ERGs are reduced in the right eye. At the 1 year follow-up examination, the multifocal ERGs have improved but are still reduced especially from the temporal retina. Shorter duration protocol with 61 hexagonal elements was used for the latest recording, because acceptable responses to 103 hexagonal elements could not be obtained due to fatigue of the patient during the recording.
Abbreviations: OD, right eye; OS, left eye.

of the enlarged blind spot. She was diagnosed with AZOOR because of ERG abnormalities. Serum anti-recoverin was negative, which was helpful to reduce the possibility that she had cancer-associated retinopathy. Irregularities in the IS/OS line of the photoreceptors were observed by OCT. The findings of OCT helped make the diagnosis.

It is known that a delayed latency of the pattern VEPs is not a specific sign of optic neuropathy because it is also found

in eyes with retinal diseases.[11–15] However, there were few reports of AZOOR showing abnormal VEPs. Gass reported that 80% of AZOOR patients had normal VEPs, and only one patient with poor visual acuity of 20/70 in the right eye and 20/300 in the left eye had abnormal VEPs.[1] Takai et al reported five AZOOR patients who had no delay in the VEPs.[7] Patients of AZOOR who had normal pattern VEPs with normal visual acuity have been reported.[16,17] Although significant abnormalities of the VEPs have rarely been reported in eyes with AZOOR, our case showed that AZOOR can be associated with significantly delayed VEPs. The mechanisms for the altered pattern VEPs without a decrease in the visual acuity was not determined in our case. The delayed VEP might be explained by reduced macular sensitivities. However, the possibility of inner retina or optic nerve involvement cannot be completely excluded.

Gass et al reported that in the presence of normal fundi, the most frequent misdiagnosis was retrobulbar neuritis, and there was a median of 17 months delay in the diagnosis of AZOOR.[2] In addition to the afferent pupillary defect, abnormal VEPs could mislead the ophthalmologist to a diagnosis of optic nerve disease. This case report serves to alert the ophthalmologist to consider the diagnosis of AZOOR and consider recording ERGs in individuals presenting with unexplained scotoma, particularly where photopsia are a prominent feature.

It has been reported that the natural course of AZOOR is varied.[2,3] Gass et al reported that visual field loss stabilized within 6 months in 37 patients (72%), progressed stepwise in two patients (4%), and partly improved in 12 patients (24%).[2] Degenerations of the photoreceptor outer segment have been detected by OCT at the convalescent stage.[6–9] There are few detailed reports about the clinical course of AZOOR patients who show some recovery. Yasuda et al reported a case with mild improvement of the multifocal ERGs, but morphological changes were not demonstrated in the report.[18] Spaide et al reported restoration of the IS/OS line in the areas of improved visual field, but electrophysiological alterations of these patients were not demonstrated in the report.[9]

Our case had a recovery of retinal function as assessed by not only visual field tests, but also full-field ERGs and multifocal ERGs. Morphological improvements were confirmed by OCT in parallel. Although it is difficult to compare the order or degree of improvement of each parameter, our case demonstrated that subjective and objective functional recovery could occur in the eyes with AZOOR. The irregular IS/OS line at the onset might have reflected incomplete loss of photoreceptor. In this case, the incomplete impairment of photoreceptor might have been associated with the visual function recovery. Further studies are needed.

Conclusion

We reported a case of AZOOR showing profoundly abnormal pattern VEPs at the onset, and significant functional recovery in the natural course. ERG findings are crucial for differentiating AZOOR from retrobulbar neuritis, especially in patients with abnormal pattern VEPs. The pattern VEPs, full-field ERGs, multifocal ERGs, and OCT images can be abnormal in the early phase of AZOOR, but they can all improve during the natural course. Further studies and long-term follow-up are needed to better understand this disorder, and these findings will hopefully reduce the number of misdiagnoses and unnecessary treatments.

Disclosure

The authors report no conflicts of interest in this work.

References

1. Gass JDM. Acute zonal occult outer retinopathy. *J Clin Neuroophthalmol.* 1993;13(2):79–97.
2. Gass JD, Agarwal A, Scott IU. Acute zonal occult outer retinopathy: a long-term follow-up study. *Am J Ophthalmol.* 2002;134(3):329–339.
3. Monson DM, Smith JR. Acute zonal occult outer retinopathy. *Surv ophthalmol.* 2011;56(1):23–35.
4. Jacobson SG, Morales DS, Sun XK, et al. Pattern of retinal dysfunction in acute zonal occult outer retinopathy. *Ophthalmology.* 1995;102(8):1187–1198.
5. Francis PJ, Marmescu A, Fitzke FW, Bird AC, Holder GE. Acute zonal occult outer retinopathy: towards a set of diagnostic criteria. *Br J Ophthalmol.* 2005;89(1):70–73.
6. Fujiwara T, Imamura Y, Giovinazzo VJ, Spaide RF. Fundus autofluorescence and optical coherence tomographic findings in acute zonal occult outer retinopathy. *Retina.* 2010;30(8):1206–1216.
7. Takai Y, Ishiko S, Kagokawa H, Fukui K, Takahashi A, Yoshida A. Morphological study of acute zonal occult outer retinopathy by multiplanar optical coherence tomography. *Acta Ophthalmol.* 2009;87(4):408–418.
8. Li D, Kishi S. Loss of photoreceptor outer segment in acute zonal occult outer retinopathy. *Arch Ophthalmol.* 2007;125(9):1194–1200.
9. Spaide RF, Koizumi H, Freund KB. Photoreceptor outer segment abnormalities as a cause of blind spot enlargement in acute zonal occult outer retinopathy-complex diseases. *Am J Ophthalmol.* 2008;146(1):111–120.
10. Optic Neuritis Study Group. The clinical profile of acute optic neuritis. Experience of the Optic Neuritis Treatment Trial. *Arch Ophthalmol.* 1991;109(12):1673–1678.
11. Lennerstrand G. Delayed visual evoked cortical potentials in retinal disease. *Acta Ophthalmol.* 1982;60(4):497–504.
12. Bass SJ, Sherman J, Bodis-Wollner I, Nath S. Visual evoked potentials in macular disease. *Invest Ophthalmol Vis Sci.* 1985;26(8):1071–1074.
13. Negishi C, Takasoh M, Fujimoto N, Tsuyama Y, Adachi-Usami E. Visual evoked potentials in relation to visual acuity in macular disease. *Acta Ophthalmol Scand.* 2001;79(3):271–276.

14. Shimada Y, Adachi-Usami E, Murayama K. How are macular changes reflected in pattern visually evoked cortical potentials? *Acta Ophthalmol Scand*. 1997;75(3):277–280.
15. Holder GE. Electrophysiological assessment of optic nerve disease. *Eye (Lond)*. 2004;18(11):1133–1143.
16 Lee AG, Prager TC. Acute zonal occult outer retinopathy. *Acta Ophthalmol Scand*. 1996;74(1):93–95.
17. Arai M, Nao-i N, Sawada A, Hayashida T. Multifocal electroretinogram indicates visual field loss in acute zonal occult outer retinopathy. *Am J Ophthalmol*. 1998;126(3):466–469.
18. Yasuda K, Shimura M, Noro M, Nakazawa M, Tamai M. Clinical course of acute retinal zonal occult outer retinopathy in visual field and multifocal electroretinogram. *Br J Ophthalmol* 1999;83(9):1089–1090.

Photoreceptor and Post-Photoreceptoral Contributions to Photopic ERG a-Wave in Rhodopsin P347L Transgenic Rabbits

Rika Hirota,[1,2] *Mineo Kondo,*[3] *Shinji Ueno,*[1] *Takao Sakai,*[1] *Toshiyuki Koyasu,*[1] *and Hiroko Terasaki*[1]

Purpose. The a-wave of the photopic electroretinogram (ERG) of macaque monkeys is made up of the electrical activities of cone photoreceptors and post-photoreceptoral neurons. However, it is not known whether the contributions of these two components change in retinas with inherited photoreceptor degeneration. The purpose of this study was to determine the contributions of cones and post-photoreceptoral neurons to the a-wave of the photopic ERGs in rhodopsin Pro347Leu transgenic (Tg) rabbits.

Methods. Ten Tg and 10 wild-type (WT) New Zealand White rabbits were studied at 4 and 12 months of age. The a-waves of the photopic ERGs were elicited by xenon flashes of different stimulus strengths before and after the activities of post-photoreceptoral neurons were blocked by intravitreal injections of a combination of 0.2 to 0.4 mM of 6-cyano-7-nitrouinoxaline-2,3(1H,4H)-dione, disodium (CNQX) and 2 to 4 mM of (±)-2-amino-4-phosphonobutyric acid.

Results. The percentage contribution of the cone photoreceptors to the photopic ERG a-waves increased with increasing stimulus strength, and the percentage ranged from 54% to 75% in 4-month-old WT rabbits. In contrast, the percentage contribution of the cone photoreceptors in 4-month-old Tg rabbits ranged from 32% to 51% ($P < 0.05$). The mean percentage contribution of cone photoreceptors became still smaller at 11% to 48% in 12-month-old Tg rabbits.

Conclusions. These results suggest that the relative contribution of cone photoreceptors to the photopic ERG a-wave is smaller in retinas with inherited photoreceptor degeneration. This indicates that the a-waves of the photopic ERGs in patients with retinitis pigmentosa must consider this lower contribution from the cone photoreceptors. (*Invest Ophthalmol Vis Sci.* 2012;53:1467–1472) DOI:10.1167/iovs.11-9006

The electroretinogram (ERG) is a mass electrical potential change of the retina that is elicited by light stimulation and is easily recorded noninvasively with a corneal electrode.[1] The ERG arises from the neural activity of the different types of retinal cells, and it can be used to perform a layer-by-layer study of retinal function in patients and animals.[2]

The origins of the photopic or light-adapted a-wave of the ERG in macaque monkeys was studied by Sieving et al.[3–5] They injected glutamate agonists and antagonists intravitreally to dissect the retinal circuits They found that the a-wave of the photopic ERG received contributions not only from the cone photoreceptors but also from post-photoreceptoral neurons (e.g., OFF-bipolar cells and horizontal cells)[3,4] because *cis*-2,3-piperidine dicarboxylic acid (PDA) or kynurenic acid reduced the a-wave amplitude. A later study by Robson et al.[6] showed that the PDA-sensitive post-photoreceptoral a-wave component started at much earlier times of approximately 5 ms in macaques. Frieberg et al.[7] also estimated the time course of the cone photoreceptor response in normal human ERGs using the paired-flash technique, in which an intense "probe" flash was delivered at different times after a "test" flash. Their results showed that the photopic ERG a-wave of the human ERG contains an appreciable postphotoreceptoral component, similar to that reported in monkeys.[3–6]

These studies, which were designed to determine the origins of the photopic ERG a-wave, have been performed primarily on normal macaque monkeys and human eyes.[3–7] It is not known whether the contributions of photoreceptors and post-photoreceptoral neurons are altered in retinas with inherited photoreceptor degeneration (e.g., retinitis pigmentosa [RP]) because the most commonly used RP animals are mice and rats, whose amplitude of photopic ERG a-wave is very small. This makes it difficult to quantify the changes in the a-wave amplitude before and after intravitreal injection of pharmacologic agents.[8–12]

We have recently succeeded in generating a rabbit model of retinal degeneration.[13] This animal has the rhodopsin Pro347Leu mutation, which is one of the major mutations in autosomal dominant retinitis pigmentosa in humans.[14] These animals have a slowly progressive photoreceptor degeneration, as do human RP patients with this mutation,[13,15–18] though it is still unclear whether the retinal degeneration is due to a point mutation of the rhodopsin gene or to an overexpression of rhodopsin in these animals. We believed that this rhodopsin transgenic (Tg) rabbit can be an excellent animal model in which to study the retinal origins of the photopic ERG a-wave in RP because rabbits have a large photopic a-wave. In addition, the large size of the rabbit's eye enabled us to perform reliable intravitreal injections of pharmacologic agents.[15,16,18]

Thus, the purpose of this study was to compare the contributions of cone photoreceptors and post-photoreceptoral neurons with the a-wave of the photopic ERGs between wild-type (WT) and Tg rabbits. To accomplish this we examined the postphotoreceptoral neural activity before and after they were blocked by pharmacologic agents.

From the [1]Department of Ophthalmology, Nagoya University Graduate School of Medicine, Nagoya, Japan; the [2]Drug Safety Research Laboratories, Astellas Pharma Inc , Osaka, Japan, and the [3]Department of Ophthalmology, Mie University Graduate School of Medicine, Tsu, Japan.

Supported by Grant-in-Aid for Scientific Research B (20390480) and Grant-in-Aid for Scientific Research C (20592075) from the Ministry of Education, Culture, Sports, Science and Technology, Japan

Submitted for publication November 3, 2011, revised January 13, 2012; accepted January 14, 2012.

Disclosure **R. Hirota**, Astellas Pharma Inc. (E), **M. Kondo**, None; **S. Ueno**, None; **T. Sakai**, None, **T. Koyasu**, None, **H. Terasaki**, None

Corresponding author: Mineo Kondo, Department of Ophthalmology, Mie University Graduate School of Medicine, 2-174 Edobashi, Tsu 514-8507, Japan, mineo@clin.medic.mie-u ac.jp.

Materials and Methods

Animals

The experiments were performed on 10 Tg and 10 littermate WT New Zealand White rabbits Our techniques for generating Tg rabbits have been described in detail.[13] This study was conducted in accordance with the ARVO Statement for the Use of Animals in Ophthalmic and Vision Research. All protocols were approved by the Animal Research Review Board of Nagoya University Graduate School of Medicine (no. 23005).

ERG Recordings

Each animal was anesthetized with an intramuscular injection of 25 mg/kg ketamine and 2 mg/kg xylazine. ERGs were recorded with a bipolar contact lens electrode (GoldLens; Doran Instruments, Littleton, MA). Animals were placed in a Ganzfeld bowl and stimulated with stroboscopic stimuli (model SG-2002; LKC Technologies, Gaithersburg, MD). The full-strength stimulus was attenuated with neutral density filters in 0 5-log unit steps Photopic ERGs were recorded after 10 minutes of light adaptation, and the stimulus strength ranged from 0.2 to 2 2 log cd-s/m^2 (photopic unit), and they were presented on a rod-suppressing white background of 3 3 log scot td Signals were amplified, band pass-filtered between 0.3 to 1000 Hz, and averaged using a computer-assisted signal analysis system (MEB-9100, Neuropack, Nihon Kohden, Tokyo, Japan).

Drug Injections

Drugs and techniques for the intravitreal injections have been described in detail.[15,16,18] The drugs were dissolved in sterile PBS, and the pH was titrated to 7 4 with hydrochloric acid or sodium hydrate. The drugs were injected into the vitreous with a 30-gauge needle inserted through the pars plana approximately 1 mm posterior to the limbus.

Two types of glutamate analogs—(±)-2 amino-4-phosphonobutyric acid (APB; Sigma-Aldrich Japan, Tokyo, Japan) and 6-cyano-7-nitroquinoxaline-2,3(1H,4H)-dione (CNQX, Sigma-Aldrich Japan)—were used. APB is an agonist of the type 6 metabotropic glutamate receptor, and it blocks signal transmission between the photoreceptors and depolarizing or ON-bipolar cells.[19] CNQX is an antagonist of the α-amino-3-hydroxy-5-methyl-4-isoxazolepropionic acid/kainic acid (AMPA/KA) class of ionotropic glutamate receptors and is known to block the light responses of the hyperpolarizing or OFF-bipolar cells, horizontal cells, and all third-order retinal neurons.[20] Thus, the combination of APB and CNQX is expected to isolate the photoreceptor responses. We could not use PDA,[21] another type of antagonist of the AMPA/KA class of ionotropic glutamate receptors, because PDA was not commercially available Intravitreal concentrations were 2 to 4 mM for APB and 0 2 to 0.4 mM for CNQX, assuming that the vitreous volume of the NZW rabbit is 1.5 mL.[22] The drugs were dissolved in 0.05 mL saline

Recordings were begun approximately 60 to 90 minutes after the drug injections, and studies were completed within 3 hours Although the drug effects were reversible, we only used the rabbits that had not been used for any previous experiments.

Measurement of a-Waves

To determine the photoreceptor and post-photoreceptoral contributions to the a-wave of the photopic ERGs quantitatively, we measured the amplitude of the a-wave before and after drug administration. Before drug administration, the a-wave amplitude was measured from the baseline to the first negative trough; after it, the a-wave amplitude was measured from the baseline to the potential at the time of the a-wave peak before the drugs (Fig. 1A). Then the percentage cone photoreceptor contribution was calculated by the expression (a-wave amplitude after APB and CNQX)/(a-wave amplitude before drugs) × 100 This method has been used to determine the degree of cone photoreceptor contribution to the a-wave.[3]

Statistical Analysis

Because the data were normally distributed, unpaired Student's *t*-tests were used to determine whether the amplitude of the a-wave of WT rabbits was significantly different from that of Tg rabbits. Differences were considered to be significant when $P < 0\ 05$.

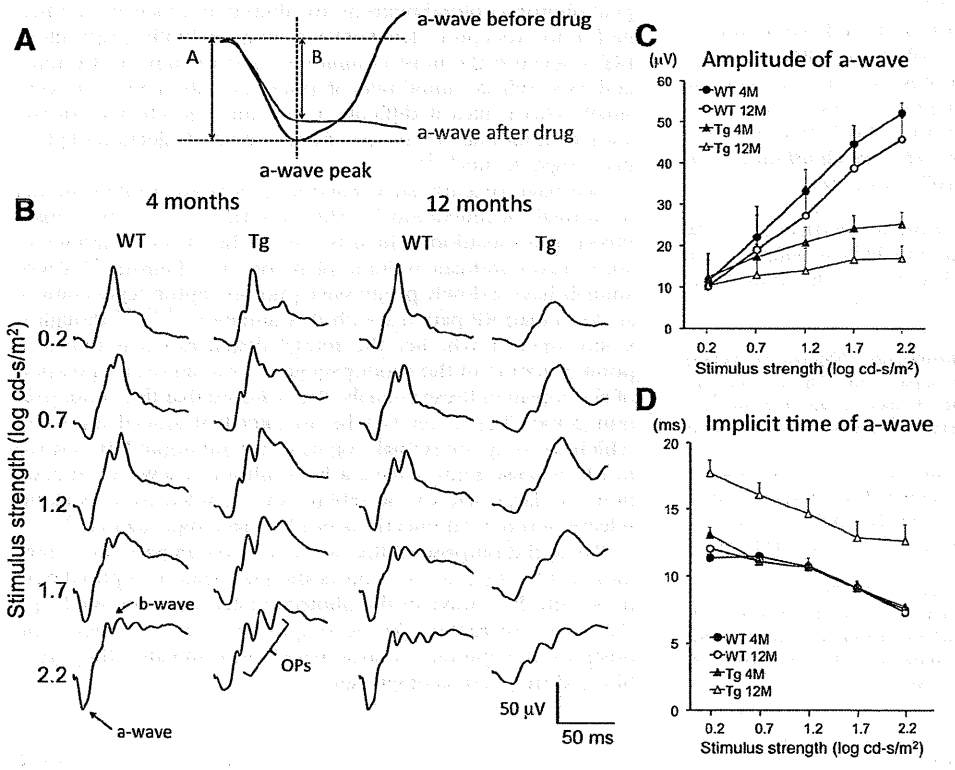

FIGURE 1. Photopic ERGs of WT and rhodopsin P347L Tg rabbits. (A) Method of measuring a-wave amplitude. The a-wave amplitude before drug administration was measured from the baseline to the first negative trough. (B) The a-wave amplitude after drug administration was measured from the baseline to the negative value at the time of the a-wave peak before drug administration. Representative photopic ERGs recorded from WT and Tg rabbits at 4 and 12 months of age. ERG waveforms to five different stimulus strengths of 0.2 to 2 2 log cd-s/m^2 are shown (C) Plots of the a-wave amplitude to five different stimulus strengths. Results of WT and Tg rabbits at 4 and 12 months of age are shown. Bars indicate the SE of the means of five animals. (D) Plots of the a-wave implicit times to five different stimulus strengths. Results of WT and Tg rabbits at 4 and 12 months of age are shown. Bars indicate the SE of the means of five animals.

Results

Photopic ERGs of WT and Tg Rabbits

Representative photopic ERGs recorded from WT and Tg rabbits at 4 and 12 months of age are shown in Figure 1B. The ERG waveforms elicited by five different stimulus strengths from 0.2 to 2.2 log cd-s/m^2 are shown. We found that all the ERG components of Tg rabbits decreased progressively with increasing age; the a-wave was more affected than the b-wave. These general ERG findings agree with the results reported in our earlier publications.[13,15]

The amplitudes of the a-waves of the photopic ERGs of Tg rabbits were significantly smaller than those of WT rabbits at 4 months of age and even smaller at 12 months of age (Figs. 1B, 1C). The implicit times of the photopic ERG a-wave were not significantly different between the Tg and WT rabbits when they were 4 months of age, but the Tg rabbits had severely delayed implicit times when they were 12 months of age (Fig. 1D).

Effect of APB or CNQX Alone on Photopic ERG a-Wave

To confirm that the a-waves of the photopic ERG in rabbits originated from the same neurons as macaque monkeys, we examined the effect of APB or CNQX alone on the a-wave of the photopic ERGs in WT and Tg rabbits when they were 4 months of age (Fig. 2). We found that intravitreal injection of APB did not alter the leading edge of the photopic a-wave, and the maximal a-wave amplitudes were nearly the same before and after the APB injection for both WT and Tg rabbits (Fig. 2, upper trace). In contrast, an intravitreal injection of CNQX significantly changed the leading edge of the a-wave, and the maximal a-wave amplitude was significantly reduced in both types of rabbits (Fig. 2, lower trace). These results were comparable to the results in primates[3–6] and support the belief that the photopic ERG a-wave receives significant contributions from post-photoreceptoral neurons, including OFF-bipolar cells and horizontal cells in both WT and Tg rabbits.

Amplitude Changes of Photopic ERG a-Wave after Pharmacologic Drug Administration

We next examined the contribution of the cone photoreceptors to the photopic ERG a-wave at the time of the a-wave peak. The black lines in Figure 3 show the photopic ERG a-waves before drugs, and the color lines (blue, WT; red, Tg) show the ERG waveforms after intravitreal injection of a solution of combined APB and CNQX (i.e., the cone photoreceptor response). The vertical dotted lines show the timing of the a-wave peaks before drug administration. As reported in primates,[3–6] the a-wave amplitude is greatly reduced after blocking all post-photoreceptoral neurons by glutamate analogs.

Mean amplitudes of the a-wave before and after drug administration at the time of the a-wave peak (Fig. 1A), are plotted in Figure 4. The a-wave amplitude decreased after injection of both APB and CNQX for all stimulus strengths in both WT and Tg rabbits.

Relative Contributions of Cone Photoreceptors to Photopic a-Wave

We next compared the relative contributions of the cone photoreceptors with the photopic ERG a-wave for the two types of rabbits. For this, we calculated the percentage contribution of the cone photoreceptors; that is, we divided the a-wave amplitude after APB+CNQX by the a-wave amplitude before drug administration (Fig. 5). We found that the percentage contribution of the cone photoreceptors became greater with increasing stimulus strengths in both WT and Tg rabbits, which is consistent with the findings in normal macaque monkeys.[3] The percentage contribution of the cone photoreceptors ranged from 32% to 51% in Tg rabbits, which was significantly smaller than that in WT rabbits at 54% to 75%, at 4 months of age ($P < 0.01$; Fig. 5, left).

We also calculated these values when the animals were 12 months of age The percentage contribution of the cone photoreceptors ranged from 11% to 48% in Tg rabbits, which was also significantly smaller than that in WT rabbits at 41% to 70% ($P < 0.05$; Fig. 5, right). The percentage contribution of cone

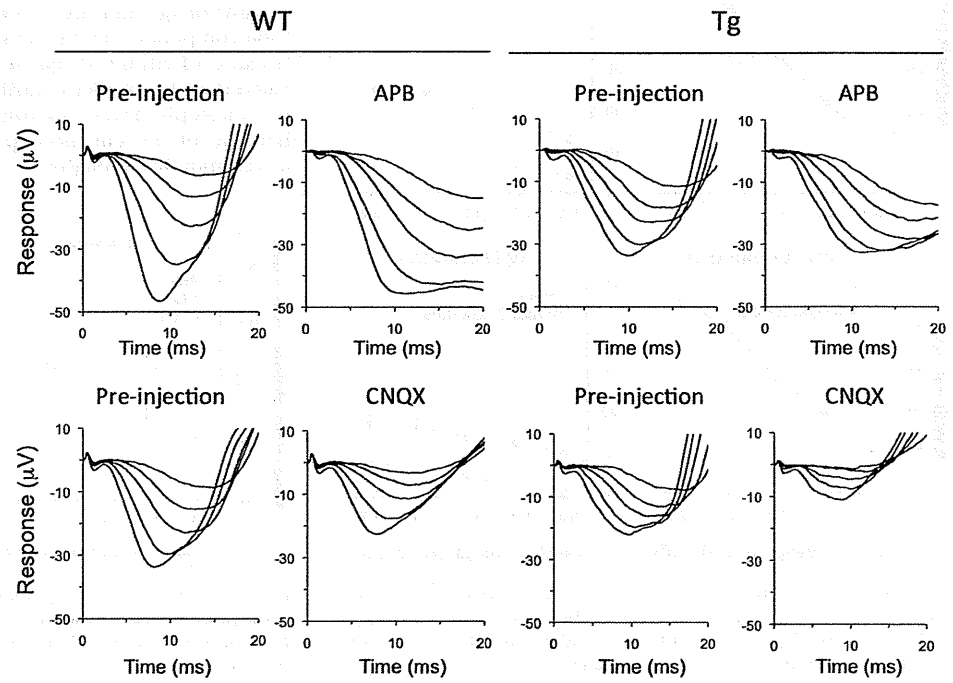

FIGURE 2. Representative waveforms of photopic ERG a-wave before and after APB or CNQX alone in WT and Tg rabbits of 4 months of age. ERG waveforms to five different stimulus strengths of 0.2 to 2 2 log cd-s/m^2 are superimposed.

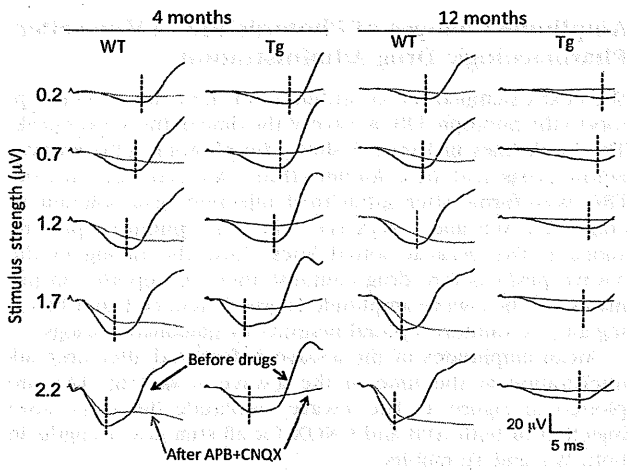

FIGURE 3. Representative waveforms of photopic ERG a-wave before (*black*) and after (*blue* and *red*) intravitreal injection of combination of APB and CNQX in WT and Tg rabbits at 4 and 12 months of age. *Vertical dotted lines*, timing of the a-wave peaks before drug administration.

photoreceptors to the photopic a-wave in 12-month-old Tg rabbits was <50% for all stimulus strengths.

Comparison of Postreceptoral Components

The smaller contributions of cone photoreceptors to the photopic a-waves in Tg rabbits can be explained simply by a decrease in cone photoreceptor responses caused by the photoreceptor degenerations, which can be clearly seen in Figure 4. However, it can also be caused by an increase in neural activities of the post-photoreceptoral neurons. To investigate whether the latter explanation was the cause, we calculated

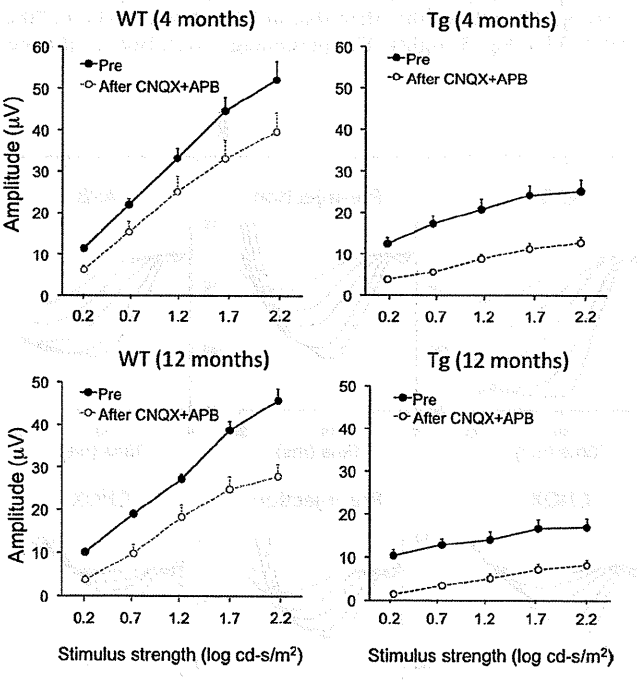

FIGURE 4. Plots of the a-wave amplitude before (*black*) and after (*blue* and *red*) intravitreal injection of combination of APB and CNQX in WT (*left*) and Tg (*right*) rabbits at 4 and 12 months of age. Bars indicate the SE of the means of five animals.

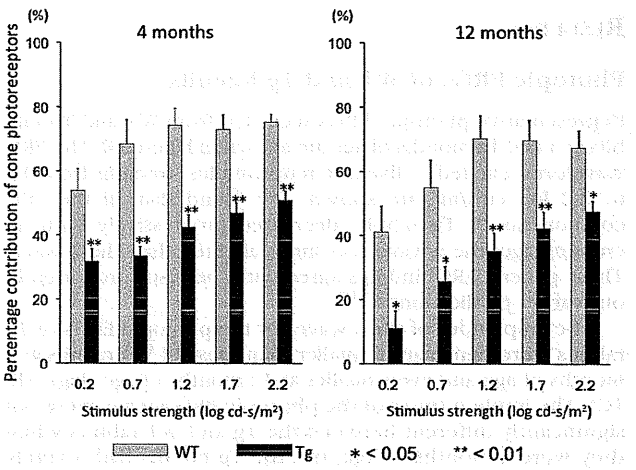

FIGURE 5. Plots of the percentage contribution of cone photoreceptors to the photopic ERG a-wave in WT (*blue*) and Tg (*red*) rabbits at 4 and 12 months of age. Bars indicate the SE of the means of five animals. $^*P < 0.05$; $^{**}P < 0.01$.

the amplitudes of post-photoreceptoral components at the time of the a-wave peak by subtracting the post-APB+CNQX waveform from the predrug waveform. Results are plotted in Figure 6.

Although the maximal amplitudes of the post-photoreceptoral components were not significantly different in WT and Tg rabbits, the intensity amplitude function for the two types of rabbits were different when they were 4 months of age (Fig. 6, left). The amplitude of the post-photoreceptoral component was nearly saturated at lower stimulus strengths of 0.7 to 1.2 log cd-s/m^2 in Tg rabbits. In contrast, this value increased gradually and reached maximum amplitude at the highest stimulus strength of 2.2 log cd-s/m^2 in WT rabbits. The amplitudes of the post-photoreceptoral components in Tg rabbits were significantly larger than those in WT rabbits at lower stimulus strengths of 0.2 and 0.7 log cd-s/m^2 ($P < 0.05$).

A similar tendency of the stimulus strength-amplitude functions of WT and Tg rabbits was also seen when they were 12 months of age, but the overall amplitudes of post-photoreceptoral components of Tg rabbits were greatly reduced, probably because of advanced retinal degeneration. These results indicated that the smaller contribution of cone photoreceptors to the photopic a-wave in young Tg rabbits occurred partially because of the enhanced post-photoreceptoral responses at lower stimulus strengths.

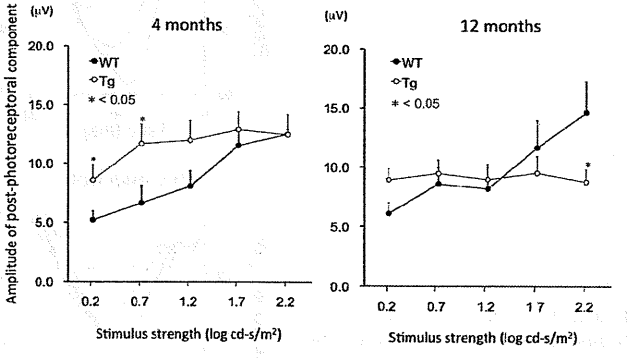

FIGURE 6. Plots of the amplitude of post-photoreceptoral component in the photopic ERG a-wave in WT (*black*) and Tg (*red*) rabbits at 4 and 12 months of age Bars indicate the SE of the means of five animals. $^*P < 0.05$.

Discussion

It is unknown whether the contributions of photoreceptors and post-photoreceptoral neurons are altered in retinas with progressive photoreceptor degeneration. Our present results clearly demonstrated that the percentage contribution of the cone photoreceptors to the photopic a-wave was significantly lower in rhodopsin P347L Tg rabbits than in WT rabbits over a 2 log unit range of stimulus strengths at both 4 and 12 months of age. We found that especially in the retina of 12-month-old Tg rabbits, the percentage contribution of cone photoreceptor to the photopic ERG a-wave was less than half, irrespective of the stimulus strength (Fig. 5, right).

Our results showed that the effects of stimulus strength on the cone photoreceptors and post-photoreceptoral contributions to the photopic a-wave of normal retinas were similar to those in primates reported by Bush and Sieving.[3] They measured the degree of cone photoreceptor and post-photoreceptoral contribution to the photopic a-wave at the time of the a-wave peak in normal macaque monkeys before and after APB and PDA. They did not report the exact percentage values, but they showed[3] that it was relatively low at 55% at the lowest stimulus strengths and that it gradually increased to a maximum of 92% at the highest stimulus strength. They interpreted these findings that the post-photoreceptoral contribution to the photopic a-wave was primarily responsible for the initial 1 to 1.5 log units of strength, whereas cone photoreceptor contribution progressively dominated the photopic a-wave at higher stimulus strengths. We also observed a similar pattern in our WT rabbits (Fig. 5), but the percentage contribution of cone photoreceptor at the highest stimulus strength was higher in macaque (92%) than in our WT rabbits (75%). This difference might have been due to the difference in the type of stimulus (200-ms long-flash stimuli in their study vs. xenon brief-flash stimuli in our study) or difference in species.

We found that the percentage contribution of cone photoreceptors to the photopic a-wave in Tg rabbits was significantly lower than in WT rabbits (Fig. 5). These results are reasonable because the cone photoreceptor is gradually attenuated whereas the middle and inner retinas are still well preserved in Tg rabbits.[13,15] Additional analyses demonstrated that the smaller percentage contribution of cone photoreceptors in young Tg rabbits can be explained, in part, by the enhancement of the amplitudes of the post-photoreceptoral component, especially at lower stimulus strengths (Fig 6, left). Such enhanced amplitudes of the post-photoreceptoral component in Tg rabbits were no longer present at 12 months in Tg rabbits, probably because of advanced retinal degeneration

We do not know the exact mechanism for the enhanced amplitudes of the post-photoreceptoral components elicited by weaker stimulus intensities in young Tg rabbits This enhanced post-photoreceptoral response may be due to secondary functional changes in the OFF-bipolar/horizontal cells or their synapses after progressive photoreceptor degenerations

Using computational molecular phenotyping, we have recently shown that during the course of rod photoreceptor degeneration, rod ON-bipolar cells switch their phenotype by expressing ionotropic glutamate receptors (iGluRs).[17] We also found that the rod bipolar cells effectively lose rod contacts and make ectopic cone contacts and express iGluRs.[17] This secondary retinal remodeling may contribute to the enhanced post-photoreceptoral responses in our Tg rabbits. Similarly, detailed ERG studies in rhodopsin P347L Tg pigs and rabbits have demonstrated that the electrical activities of the cone ON-pathway were also enhanced at a relatively early stage of retinal degeneration.[18,23] In addition, an increase in the ERG responses from the inner retina (e.g., scotopic threshold response) was also reported in the retina of the aged Royal College of Surgeons rat, a rodent model of retinal degeneration.[24,25]

Taken together, inherited retinal diseases associated with progressive photoreceptor degeneration may lead to different types of functional changes in the post-photoreceptoral retinal circuits, including the ON- and OFF pathways, during a relatively early stage of retinal degeneration.

We believe our results have important clinical implications. The a-wave of the photopic ERG is believed to be shaped primarily by electrical activities of cone photoreceptors in patients. However, the results of this study suggest that the cone photoreceptor function may be overestimated when the amplitude of the cone ERG a-wave is used as an indicator of residual cone photoreceptor functions in patients with progressive photoreceptor degeneration such as RP. Thus, when the standard stimulus strength (3.0 cd-s/m^2 = 0.48 log cd-s/m^2) recommended by the International Society of Clinical Electrophysiology of Vision[1] was used, contributions of the cone photoreceptors to the photopic a-wave was only 34% at the time of the a-wave peak, and the other 66% originated from post-photoreceptoral neurons (Fig. 5, left). Our results suggest that the lower contribution of the cones to the a-waves of the photopic ERGs must be considered in patients with RP.

There are limitations to this study. One was that we assessed the contribution of photoreceptors and post-photoreceptoral components only at the time of the a-wave peak before the drugs. However, the peak time of the a-wave depends on not only the stimulus strength but also on the presence of retinal degeneration (Fig. 1D). In addition, the a-wave can be truncated by the b-wave. To overcome this, we measured the a-wave amplitude at specific times before the b-wave intrusion (10.5 ms for 0.2 log cd-s/m^2, 9.5 ms for 0.7 log cd-s/m^2, 8.5 ms for 1.2 log cd-s/m^2, 7.5 ms for 1.7 log cd-s/m^2, and 6.5 ms for 2.2 log cd-s/m^2), and calculated the percentage cone photoreceptor contribution when the animals were 4 months of age. We found that the cone photoreceptor contribution still tended to be smaller in Tg rabbits than in WT rabbits, and the differences were significant at the two lower stimulus strengths ($P < 0.01$, Supplementary Fig. S1A, http://www.iovs.org/lookup/suppl/doi:10.1167/iovs.11-9006/-/DCSupplemental). We also measured the a-wave amplitude at a single constant time of 7 ms and calculated the percentage cone photoreceptor contribution. Again, the cone photoreceptor contribution tended to be smaller in Tg rabbits than in WT rabbits, but the difference was significant only at the highest stimulus strength (Supplementary Fig. S1B, http://www.iovs.org/lookup/suppl/doi:10.1167/iovs.11-9006/-/DCSupplemental).

In summary, our results indicate that the relative contribution of cone photoreceptors to the photopic ERG a-wave is smaller in retinas with inherited photoreceptor degeneration. These results suggest that care must be taken in interpreting the a-wave amplitudes of photopic ERGs in patients with progressive photoreceptor degeneration.

Acknowledgments

The authors thank Duco I. Hamasaki for editing the manuscript and Michael Bach for helpful discussions.

References

1. Marmor MF, Fulton AB, Holder GE, et al. ISCEV Standard for full-field clinical electroretinography (2008 update). *Doc Ophthalmol.* 2009;118:69–77.
2. Frishman LJ. Origins of the electroretinogram. In: Heckenlively JR, Arden GB, eds. *Principles and Practice of Clinical Electrophysiology of Vision* 2nd ed. London: MIT Press; 2006:139–183.
3. Bush RA, Sieving PA. A proximal retinal component in the primate photopic ERG a-wave. *Invest Ophthalmol Vis Sci.* 1994;35:635–645

4. Sieving PA, Murayama K, Naarendorp F. Push-pull model of the primate photopic electroretinogram: a role for hyperpolarizing neurons in shaping the b-wave. *Vis Neurosci.* 1994;11:519–532.
5. Jamison JA, Bush RA, Lei B, Sieving PA. Characterization of the rod photoresponse isolated from the dark-adapted primate ERG. *Vis Neurosci.* 2001;18:445–455.
6. Robson JG, Saszik SM, Ahmed J, Frishman LJ. Rod and cone contributions to the a-wave of the electroretinogram of the macaque. *J Physiol.* 2003;547.509–530.
7. Friedburg C, Allen CP, Mason PJ, Lamb TD. Contribution of cone photoreceptors and post-receptoral mechanisms to the human photopic electroretinogram. *J Physiol.* 2004;556.819–834.
8. Sharma S, Ball SL, Peachey NS. Pharmacological studies of the mouse cone electroretinogram. *Vis Neurosci.* 2005;22.631–636.
9. Bui BV, Fortune B. Origin of electroretinogram amplitude growth during light adaptation in pigmented rats. *Vis Neurosci.* 2006;23:155–67.
10. Koyasu T, Kondo M, Miyata K, et al. Photopic electroretinograms of mGluR6-deficient mice. *Curr Eye Res.* 2008;33.91–99.
11. Miura G, Wang MH, Ivers KM, Frishman LJ. Retinal pathway origins of the pattern ERG of the mouse. *Exp Eye Res.* 2009;89:49–62.
12. Shirato S, Maeda H, Miura G, Frishman LJ. Postreceptoral contributions to the light-adapted ERG of mice lacking b-waves. *Exp Eye Res.* 2008;86:914–928.
13. Kondo M, Sakai T, Komeima K, et al. Generation of a transgenic rabbit model of retinal degeneration. *Invest Ophthalmol Vis Sci.* 2009;50:1371–1377.
14. Dryja TP, Hahn LB, Cowley GS, et al. Mutation spectrum of the rhodopsin gene among patients with autosomal dominant retinitis pigmentosa. *Proc Natl Acad Sci U S A.* 1991;88:9370–9374.
15. Sakai T, Kondo M, Ueno S, et al. Supernormal ERG oscillatory potentials in transgenic rabbit with rhodopsin P347L mutation and retinal degeneration. *Invest Ophthalmol Vis Sci.* 2009;50:4402–449.
16. Yokoyama D, Machida S, Kondo M, et al. Pharmacological dissection of multifocal electroretinograms of rabbits with Pro347Leu rhodopsin mutation. *Jpn J Ophthalmol.* 2010;54:458–466.
17. Jones BW, Kondo M, Terasaki H, et al. Retinal remodeling in the Tg P347L rabbit, a large-eye model of retinal degeneration. *J Comp Neurol.* 2011;519:2713–2733.
18. Nishimura T, Machida S, Kondo M, et al. Enhancement of ON-bipolar cell responses of cone electroretinograms in rabbits with Pro347Leu rhodopsin mutation. *Invest Ophthalmol Vis Sci.* 2011;52:7610–7617.
19. Slaughter MM, Miller RF. 2-Amino-4-phosphonobutyric acid: a new pharmacological tool for retina research. *Science.* 1981;211:182–185.
20. Honoré T, Davies SN, Drejer J, et al. Quinoxalinediones: potent competitive non-NMDA glutamate receptor antagonists. *Science.* 1988;241.701–703.
21. Slaughter MM, Miller RF. An excitatory amino acid antagonist blocks cone input to sign-conserving second-order retinal neurons. *Science.* 1983;219:1230–1232.
22. Leeds JM, Henry SP, Truong L, et al. Pharmacokinetics of a potential human cytomegalovirus therapeutic, a phosphorothioate oligonucleotide, after intravitreal injection in the rabbit. *Drug Metab Dispos.* 1997;25:921–926.
23. Banin E, Cideciyan AV, Alemán TS, et al. Retinal rod photoreceptor-specific gene mutation perturbs cone pathway development. *Neuron.* 1999,23:549–557.
24. Bush RA, Hawks KW, Sieving PA. Preservation of inner retinal responses in the aged Royal College of Surgeons rat: evidence against glutamate excitotoxicity in photoreceptor degeneration. *Invest Ophthalmol Vis Sci.* 1995,36.2054–2062.
25. Machida S, Raz-Prag D, Fariss RN, et al. Photopic ERG negative response from amacrine cell signaling in RCS rat retinal degeneration. *Invest Ophthalmol Vis Sci.* 2008;49:442–452.